Electronic Supplementary Information

Superior electrocatalytic hydrogen evolution activity of a triply bridged diruthenium(II) complex on carbon cloth support

Yogita Arya,[a] Toufik Ansari,[b] Sudip Kumar Bera,[a] Sanjib Panda,[a] Arindam Indra,*[b] and Goutam Kumar Lahiri*[a]

[a]*Department of Chemistry, Indian Institute of Technology Bombay, Powai, Mumbai-400076, India. Email: lahiri@chem.iitb.ac.in*

[b] *Department of Chemistry, Indian Institute of Technology BHU, Varanasi- 221005, India. Email: arindam.chy@iitbhu.ac.in*

Experimental Section

Materials

The precursor complex $[Ru^{II}(PPh_3)_3(CO)(H)(Cl)]$[1] and free ligands L1/L2/L3[2] were prepared according to the reported literature procedures. Other chemicals and solvents were of reagent grade and used as received. For spectroscopic and electrochemical studies HPLC-grade solvents were used.

Physical measurements

Electrospray mass spectrometry (ESI-MS) was performed on Bruker's Maxis Impact (282001.00081) instrument. ^{1}H NMR were recorded on a Bruker Avance III 400 MHz spectrometer.

Cyclic and differential pulse voltammetric measurements were done using a PAR model 273A electrochemistry system. A glassy carbon working electrode, platinum wire auxiliary electrode and a saturated calomel reference electrode (SCE) were used in a standard three-electrode configuration with Et_4NClO_4 (TEAP) as the supporting electrolyte (substrate concentration ≈ 10^{-3} M; standard scan rate 100 mV s^{-1}). The half-wave potential E^o was set equal to $0.5(E_{pa}+E_{Pc})$, where E_{pa} and E_{Pc} are anodic and cathodic cyclic voltammetry peak potentials, respectively. A platinum wire guaze electrode was used for the constant potential coulometry experiment. Electrochemical hydrogen evolution activities and kinetic studies were performed using Metrohm Autolab (BCA80276).

UV-vis-NIR spectra were performed on a PerkinElmer Lambda 1050 spectrophotometer. The electrical conductivity was checked using an autoranging conductivity meter (Toshcon Industries, India). Infrared spectra were recorded on a PerkinElmer Spectrum One IR spectrophotometer with samples prepared as KBr pellets. The elemental analyses were performed on a Vario MICRO CUBE Elementar.

Preparation of complexes

Syntheses of $[(PPh_3)(CO)Ru^{II}(\mu\text{-}H)(\mu\text{-}L1)(\mu\text{-}Cl)Ru^{II}(CO)(PPh_3)](ClO_4)_2$ ([1]$(ClO_4)_2$), $[(PPh_3)_2(CO)(H)Ru^{II}(L2')]$ ([2]ClO_4) and $[(PPh_3)_2(CO)(H)Ru^{II}(L3')]$ ([3]ClO_4). Complexes [**1**]$(ClO_4)_2$, [**2**]ClO_4 and [**3**]ClO_4 were obtained from the reactions of metal precursor $[Ru^{II}(PPh_3)_3(CO)(H)(Cl)]$ (100 mg, 0.10 mmol) and the ligand L1 (20 mg, 0.05 mmol), L2 (32 mg, 0.05 mmol) and L3 (37 mg, 0.05 mmol), respectively, in refluxing EtOH for 12 h under a dinitrogen atmosphere. The residue thus obtained in each case on removing the solvent under reduced pressure was moistened with a few drops of CH_3CN. A saturated aqueous solution of $NaClO_4$ was then added into it, and the solution was allowed to cool overnight at 273 K. The precipitate was filtered off, washed with chilled water to remove excess $NaClO_4$ and dried under vacuum over P_4O_{10}. The product was purified on a neutral alumina column with a CH_2Cl_2/CH_3CN (3:2) mixture as an eluant. The pure complexes were obtained on removal of solvent under reduced pressure.

[1]$(ClO_4)_2$: Yield: 52 mg (70%). MS (ESI+, CH_3CN): *m/z* calcd for $\{([\mathbf{1}](ClO_4)_2)\text{-}ClO_4\}^+$: 1307.08; found: 1307.06. ^{1}H NMR (400 MHz, $(CD_3)_2SO$): δ = 9.33 (d, *J* = 7.3 Hz, 1H), 9.26 (d, *J* = 5.7 Hz, 1H), 8.95 (m, 2H), 8.66 (d, *J* = 8.3 Hz, 1H), 8.21 (d, *J* = 7.9 Hz, 2H), 8.04 (t, *J* = 8.2 Hz, 2H), 7.68 (t, *J* = 8.0 Hz, 1H), 7.54 (m, 3H), 7.42 (t, *J* = 8.1 Hz, 3H), 7.24 (m, 18H), 6.94 (m, 12H), -16.19 (dd, *J* = 20 Hz, 1H) ($^2J_{P\text{-}H}/Hz$: 20) ppm. ^{31}P NMR (162 MHz, $CDCl_3$): δ = 59, 40ppm. Molar conductivity (CH_3CN): Λ_M = 202 Ω^{-1} cm^2 M^{-1}. Anal. Calcd for $C_{62}H_{47}Cl_2N_6O_{10}P_2Ru_2$: C, 54.50; H, 3.46; N, 6.13; found: C, 54.56; H, 3.81; N, 6.11. IR (KBr, cm^{-1}): 1985 [ν(C≡O)], 1091 [$\nu(ClO_4^-)$] and 1632 [ν(Ru-H-Ru)].

[2]ClO_4: Yield: 65 mg (57%). MS (ESI+, CH_3CN): *m/z* calcd for $\{([\mathbf{2}]ClO_4)\text{-}ClO_4\}^+$: 997.23; found: 997.21. ^{1}H NMR (400 MHz, $CDCl_3$): δ = 9.74 (d, *J* = 8.0 Hz, 1H), 8.70 (d, *J* = 8.7 Hz, 1H), 7.96 (t, *J* = 7.8 Hz, 1H), 7.80 (m, 2H), 7.68 (m, 2H), 7.39 (m, 18H), 7.26 (m, 12H), 7.04 (d, *J* = 7.8 Hz, 1H), 6.96 (d, *J* = 7.9, 1H), 2.66 (s, 3H), 2.42 (s, 3H), 2.17 (s, 3H), -

14.06 (t, 1H) ($^2J_{P\text{-}H}/Hz$: 36) ppm. ^{31}P NMR (162 MHz, $CDCl_3$): δ = 44.16 ppm. Molar conductivity (CH_3CN): Λ_M = 98 Ω^{-1} cm^2 M^{-1}. Anal. Calcd for $C_{58}H_{49}ClN_4O_6P_2Ru$: C, 63.53; H, 4.50; N, 5.11; found: C, 63.27; H, 4.34; N, 5.27. IR (KBr, cm^{-1}): 1935 [ν(C≡O)], 1093 [ν(ClO_4^-)].

[3]ClO$_4$: Yield: 81 mg (60%). MS (ESI+, CH_3CN), *m/z* calcd for {([**3**]ClO_4)-ClO_4}$^+$: 1192.91; found: 1192.14. ^{1}H NMR (400 MHz, $CDCl_3$): δ = 7.95 (d, *J* = 8.6 Hz, 2H), 7.47 (t, *J* = 8.2 Hz 3H), 7.32 (m, 4H), 7.17 (m, 18H), 7.02 (m, 12H), 6.31 (d, *J* = 7.7 Hz, 1H), -12.03 (t, 1H) ($^2J_{P\text{-}H}/Hz$: 36) ppm. ^{31}P NMR (202 MHz, $CDCl_3$): δ = 42.05 ppm. Molar conductivity (CH_3CN): Λ_M = 102 Ω^{-1} cm^2 M^{-1}. Anal. Calcd for $C_{55}H_{40}ClBr_3N_4O_6P_2Ru$: C, 51.16; H, 3.12; N, 4.34; found: C, 51.34; H, 3.34; N, 4.47. IR (KBr, cm^{-1}): 1937 [ν(C≡O)], 1090 [ν(ClO_4^-)].

Caution! Perchlorate salts are potentially explosive and should be handled with care.

Preparation of the working anode

3 mg catalyst was dissolved in 60 µL dichloromethane and the solution was drop casted on 1 x 1 cm^{-2} area of CC (carbon cloth) by a micropipette (3 x 20 µL) and dried for 1 h in an air oven at 60°C.

Electrochemical experiments

The electrochemical studies were carried out in a single-compartment three-electrode setup immersed in aqueous phosphate buffer solution with different pH values (pH = 3, 7 and 12). The working electrode was carbon cloth supported catalyst, while platinum wire and Ag/AgCl were used as counter and reference electrodes, respectively. The linear sweep voltammetry (LSV) was presented with 60% i*R* correction. The following equation was used to reference each potential against the reversible hydrogen electrode:

$E_{RHE} = E_{Ag/AgCl} + 0.197 + 0.059$ pH

The EIS spectra were collected with an anodic polarisation potential of 1.45 V *versus* RHE. The frequency range of measurement were 0.01 to 106 Hz.

Photoelectrochemical measurements

Photoelectrochemical studies were conducted using fluorine-doped tin oxide (FTO) as the conducting support. Initially, 1 mg of [**1**]$(ClO_4)_2$ was dissolved in dichloromethane (DCM) and deposited on FTO by drop-casting. Here also, single-compartment three-electrode setup immersed in a phosphate buffer solution was used. LED light (X001O8ZOBF) was used as the illumination source for the photoelectrochemical measurements.

Optimization of the catalyst loading

The amount of catalyst loading was optimized for **[1]**$(ClO_4)_2$ and same amount was loaded for [**2**]ClO_4/[**3**]ClO_4 irrespective of their molecular weight. The loading of [**1**]$(ClO_4)_2$ on carbon cloth was optimized based on two factors:

(i) High HER activity and (ii) the limit of catalyst loading on 1 x1 cm^2 area of carbon cloth. With increasing amount of catalyst loading (1-4 mg) on CC, HER activity increased up to 3 mg of loading. No improvement of activity was observed on excess loading, In addition, higher loading crossed the limit of carbon cloth to hold the catalyst on it, causing leaching and inhomogeneous distribution of the catalyst onto the support.

Loading and characterisation of the catalysts

The loading of catalyst was 3 mg cm^{-2}. The weight difference of the carbon cloth before and after the catalyst loading ensured the loading of the catalyst on the support. The error was estimated to be in the range of 3±0.1 mg. Further, retention of the molecular entity of the complex on the carbon cloth support was identified by PXRD as well as by the unaltered UV-vis spectrum of the redissolved catalyst. The homogeneous distribution of the catalyst on carbon cloth support was ascertained by SEM experiment.

Recovery of the catalyst

Catalyst was successfully recovered after the catalytic process. To recover the catalyst, carbon cloth with deposited catalyst was immersed in dichloromethane to make it soluble.

Subsequently, UV-visible spectrum of the recovered catalyst was recorded.

After the HER process, catalyst@carbon cloth was washed with water, dried in oven (60 ^{o}C for 12 h), and measured the weight. 10% decrease in weight of the catalyst@carbon cloth was observed. Additionally, UV-vis spectrum showed 88% retention of the catalyst on the support after HER process.

Crystal structure determination

Single crystals were obtained by slow evaporation of a 1:1 $CHCl_3$:C_6H_6 solution of L3 and [**1**]$(ClO_4)_2$, 1:1 $CHCl_3$:Toluene solution of [**2**]ClO_4 and 1:1 $CHCl_3$:C_6H_6 solution of [**3**]ClO_4. X-ray diffraction data were collected using a Bruker D8 QUEST single crystal diffractometer using Mo-Kα radiation at 150(2) K. The data collection was evaluated using the CrystalClear-SM Expert software. The data were collected by the standard ω-scan technique. The structure was solved by direct methods using SHELXL-2018 and refined by full matrix least-squares with SHELXL-2018, refining on F^2.[3] All data were corrected for Lorentz and polarisation effects and all non-hydrogen atoms were refined anisotropically. The remaining hydrogen atoms were placed in geometrically constrained positions and refined with isotropic temperature factors, generally 1.2U_{eq} of their parent atoms. Hydrogen atoms were included in the refinement process as per the riding model. CCDC nos. 2323104, 2311897, 2311898, 2311899 contain the supplementary crystallographic data for L3, [**1**]$(ClO_4)_2$, [**2**]ClO_4 and [**3**]ClO_4 respectively. These data can be obtained free of charge from the Cambridge crystallographic data centre via www.ccdc.cam.ac.uk/data_request/cif.

Computational details

Full geometry optimisations were carried out using the density functional theory method at (U)B3LYP/LanL2DZ/6-31G* level for $\mathbf{1}^n$ (n = +3, 1, 0), $\mathbf{2}^n$ (n = +2, 0), $\mathbf{3}^n$ (n = +2, 0, –1) and (R)B3LYP for $\mathbf{1}^n$ (+2), $\mathbf{2}^n$/$\mathbf{6}^n$ (n = +1).[4] All elements except ruthenium was assigned the 6-31G***** basis set. The LanL2DZ basis set with effective core potential was employed for the

ruthenium atom.[5] Vertical electronic excitations based on (B3LYP/LanL2DZ/6-31G*) optimized geometries were computed using the time-dependent density functional theory (TD-DFT) formalism[6] in acetonitrile using the conductor-like polarizable continuum model (CPCM).[7] Electronic spectra were calculated using the SWizard program.[8] Chemissian 1.7[9] was used to calculate the fractional contributions of various groups to each molecular orbital. All calculated structures were visualized with ChemCraft.[10]

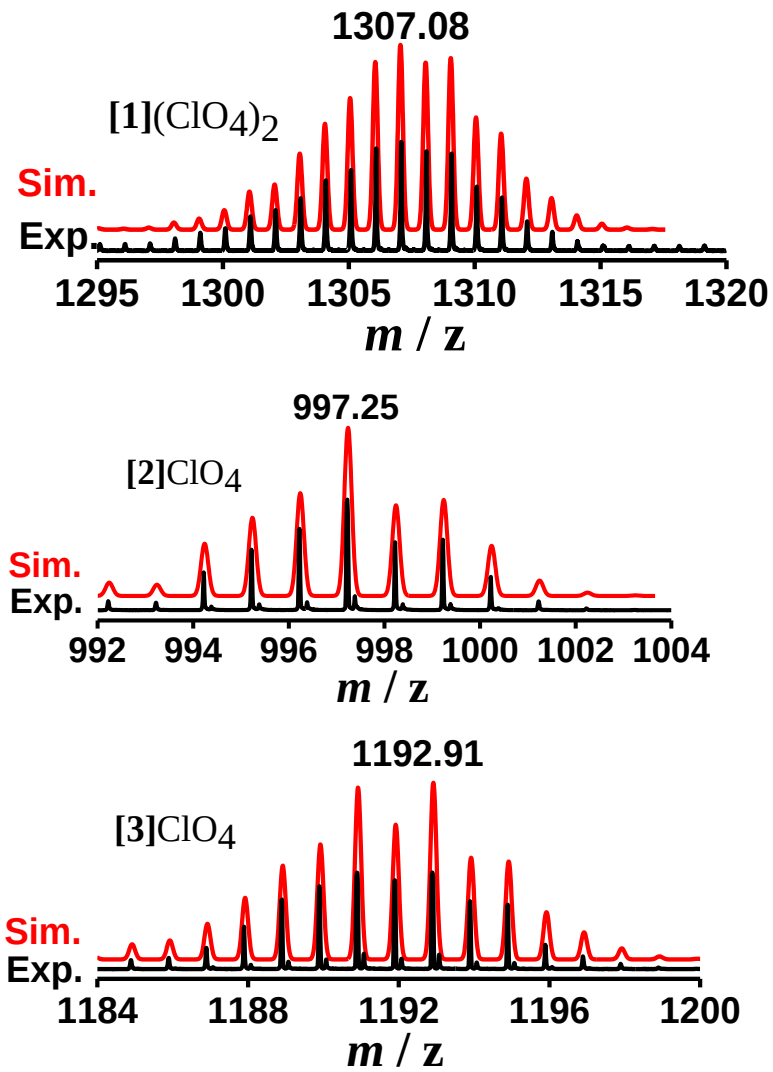

Fig. S1 Mass spectra of the complexes.

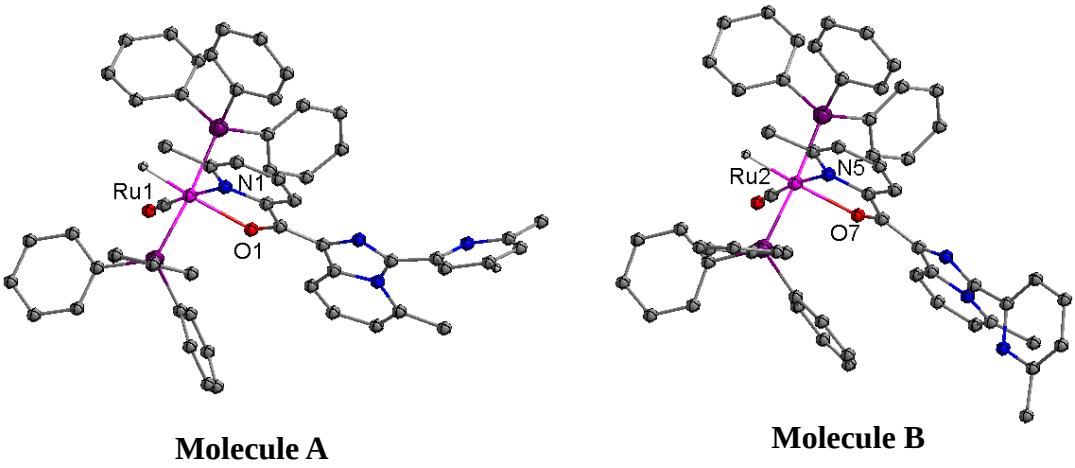

Fig. S2 Perspective views of the cationic part of [**2**]ClO_4. Ellipsoids are drawn at 30% probability level. Hydrogen atoms except Ru-H and ClO_4^- are omitted for clarity.

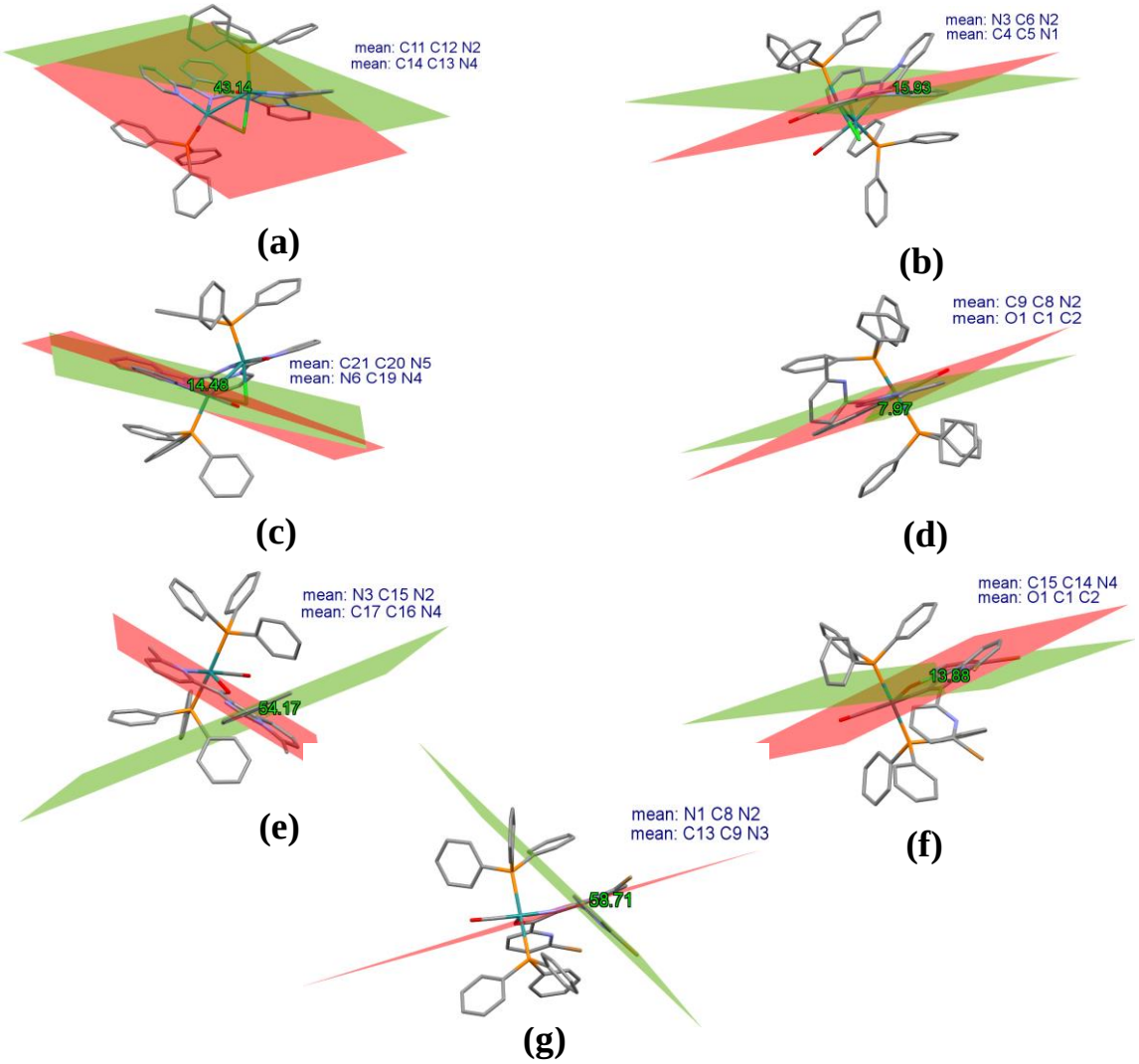

Fig. S3 Torsional angles (deg) between the planes for (a)/(b)/(c) for [**1**]$(ClO_4)_2$, (d)/(e) [**2**]ClO_4 and (f)/(g) for [**3**]ClO_4.

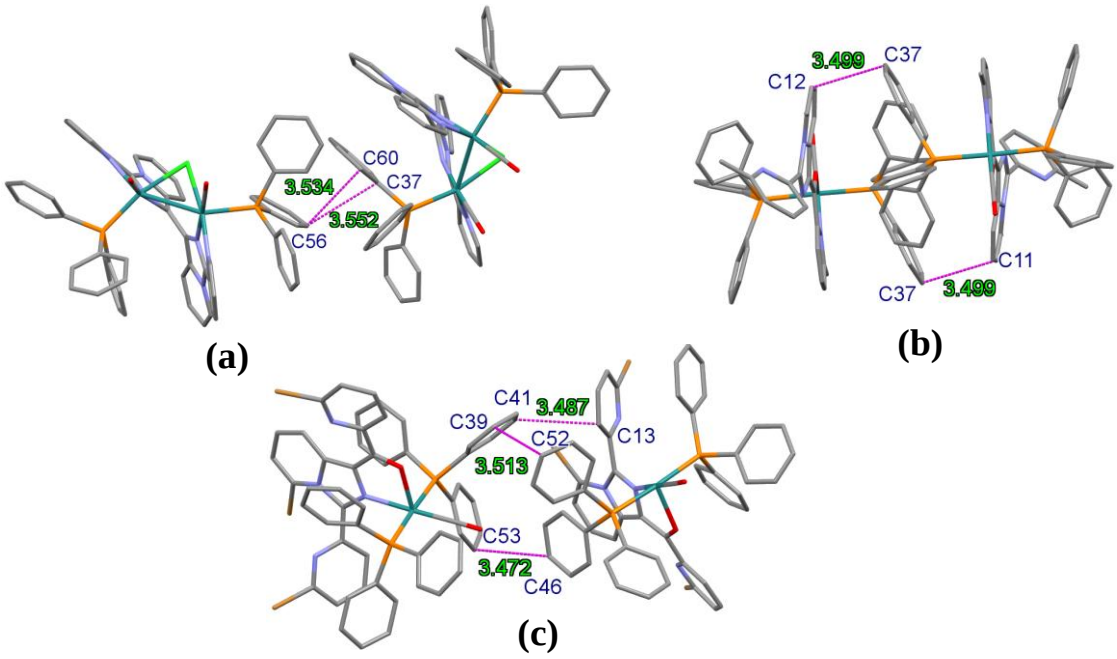

Fig. S4a π---π interactions between the neighbouring molecules for (a) [**1**]$(ClO_4)_2$, (b) [**2**]ClO_4 and (c) [**3**]ClO_4.

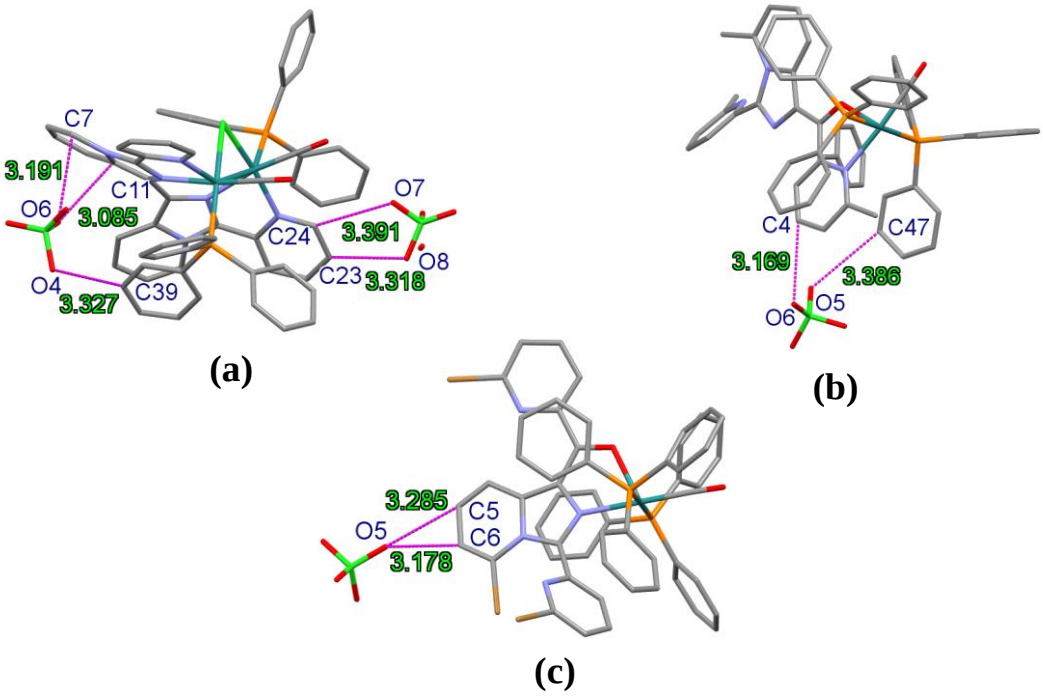

Fig. S4b C-H---O hydrogen bonding interactions between the neighbouring molecules of (a) [**1**]$(ClO_4)_2$, (b) [**2**]ClO_4 and (c) [**3**]ClO_4.

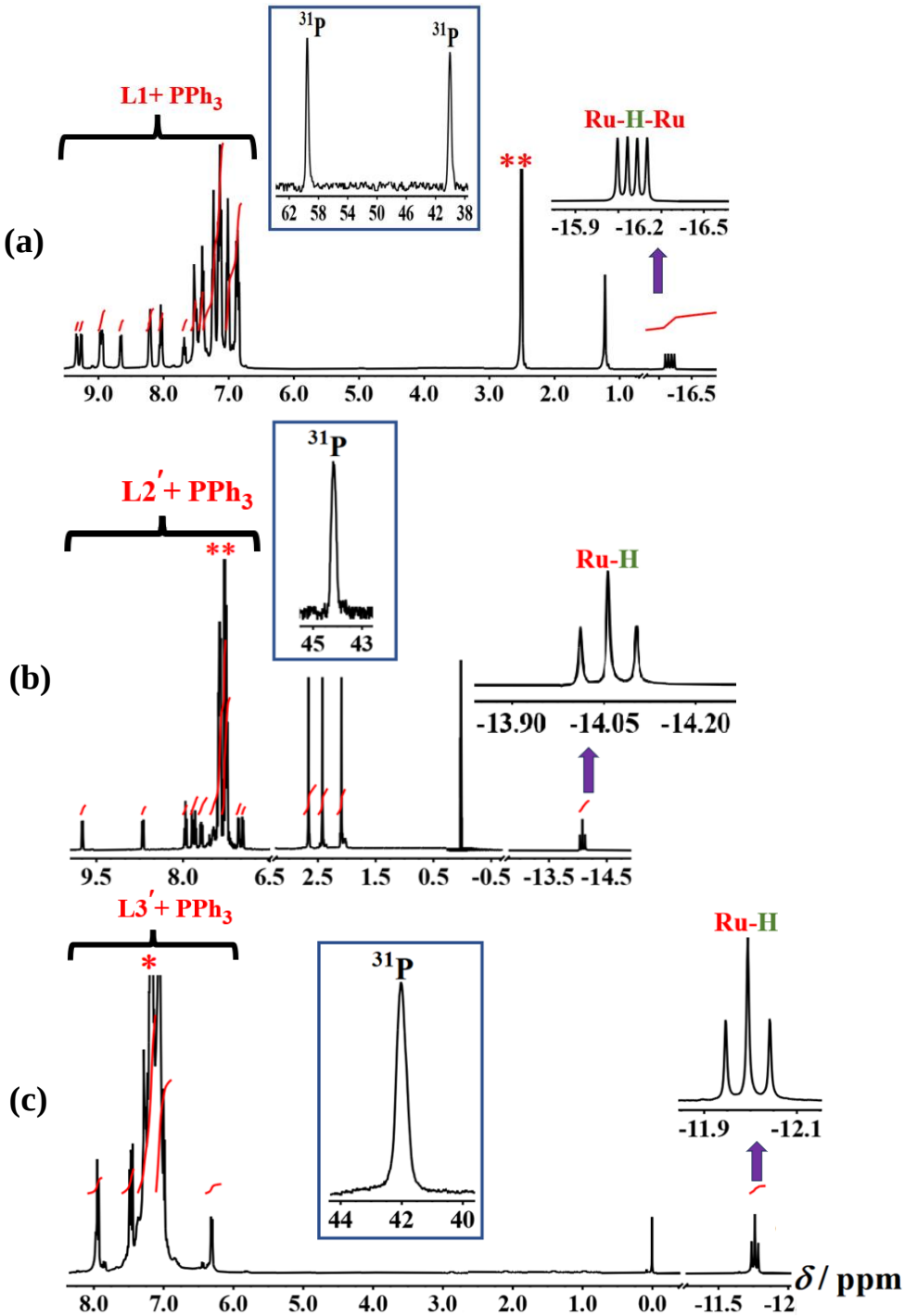

Fig. S5 ^{1}H NMR spectra of (a) [**1**]$(ClO_4)_2$, (b) [**2**]ClO_4 and (c) [**3**]ClO_4 in $(CD_3)_2SO$ (**) and $CDCl_3$ (*), respectively, with TMS (δ = 0 ppm) as an internal standard. Inset shows segmented ^{31}P NMR signature of complexes.

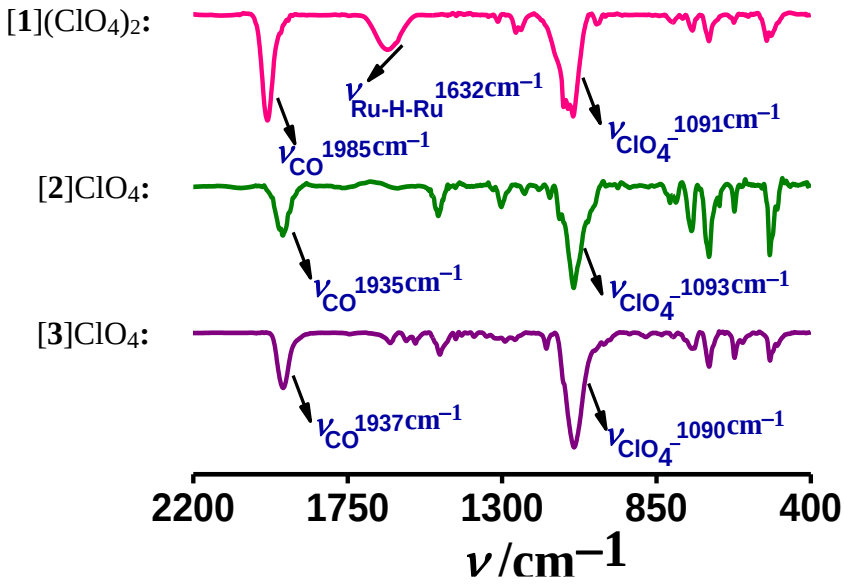

Fig. S6 IR spectra as KBr disc.

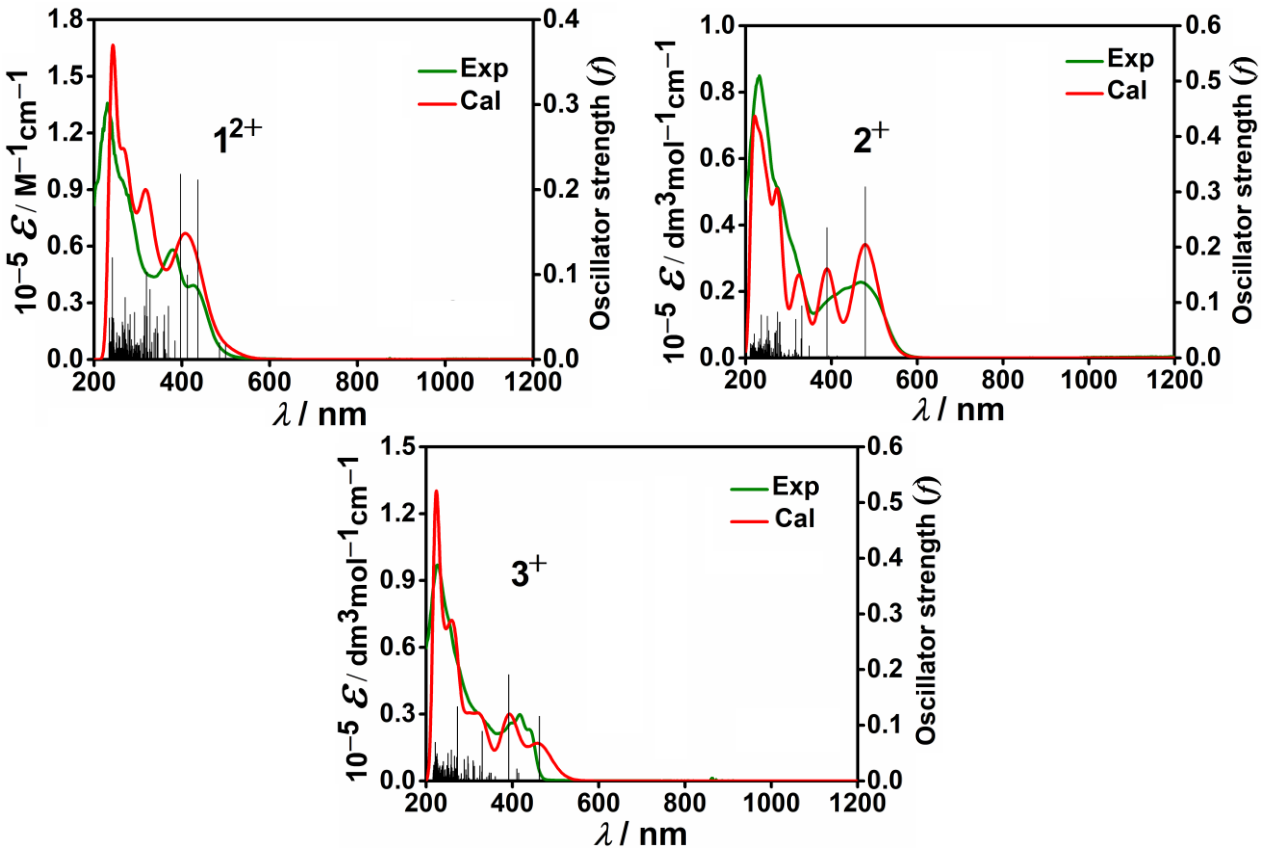

Fig. S7 Experimental and TD-DFT (B3LYP/(CPCM)/LanL2DZ/6-31G*) calculated electronic spectra in CH_3CN. Oscillator strengths are shown by black vertical lines; the spectra (red) are convoluted with a Gaussian function having fullwidth at half-maximum of 3000 cm^{-1}.

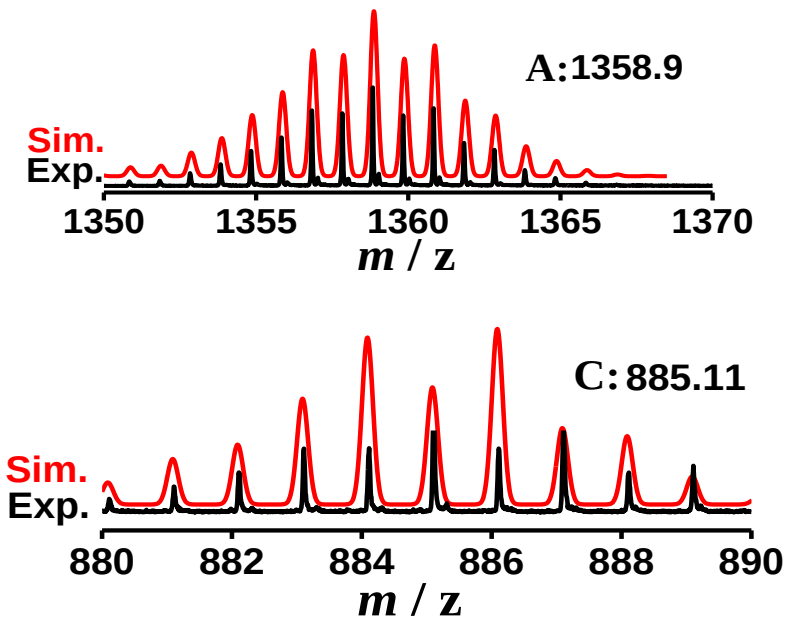

Fig. S8a Mass spectrometry of (a) **A** and (b) **D**.

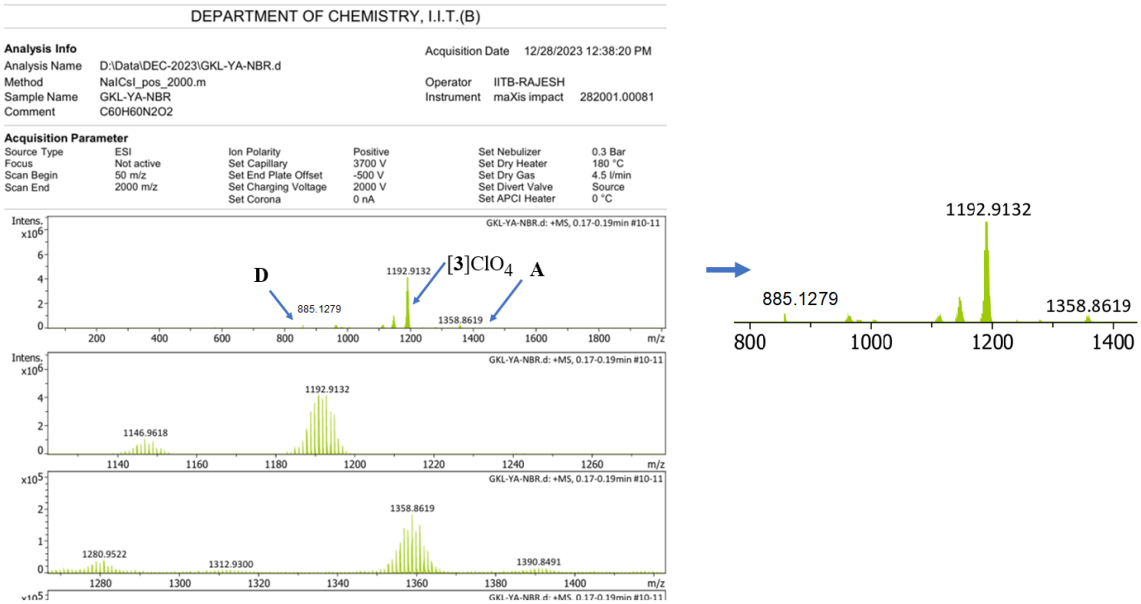

Fig. S8b Mass spectrum of crude [**3**]ClO_4.

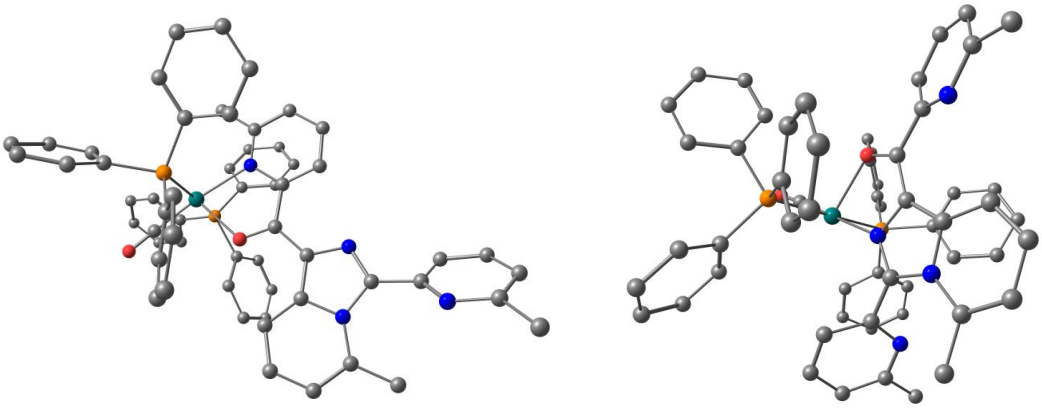

(a) **(b)**

Fig. S9a (a) N,O piconyl (energy = –2124526.64 kcal/mol) binding mode of [**2**]ClO_4 and (b) N(imidazopyridine)/O(piconyl) (energy = –2124524.76 kcal/mol) binding mode of [**2**]ClO_4.

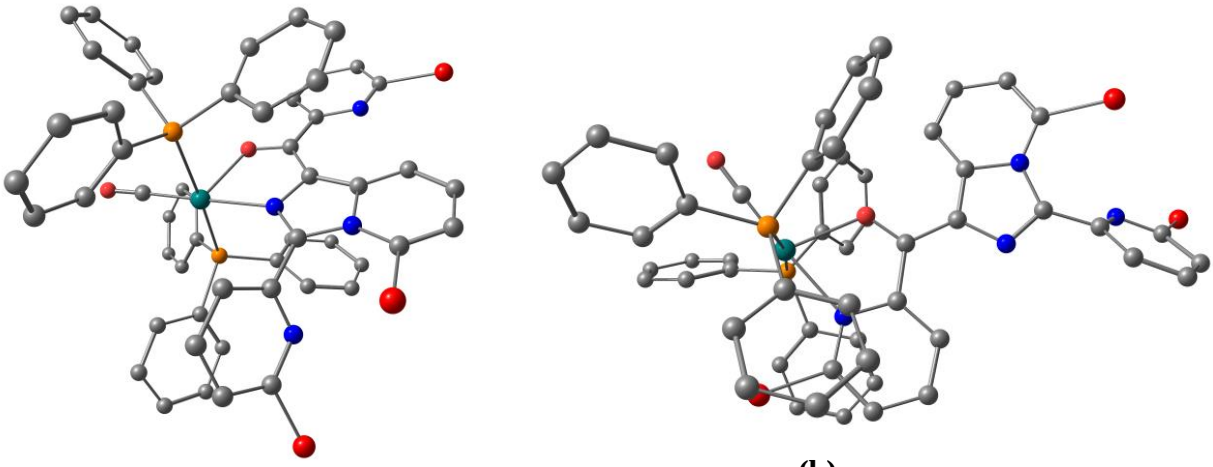

(a) **(b)**

Fig. S9b (a) N(imidazopyridine)/O(piconyl) (energy = –6890104.002 kcal/mol) binding mode of [**3**]ClO_4 and (b) N,O piconyl (energy = –6890101.304 kcal/mol) binding mode of [**3**]ClO_4.

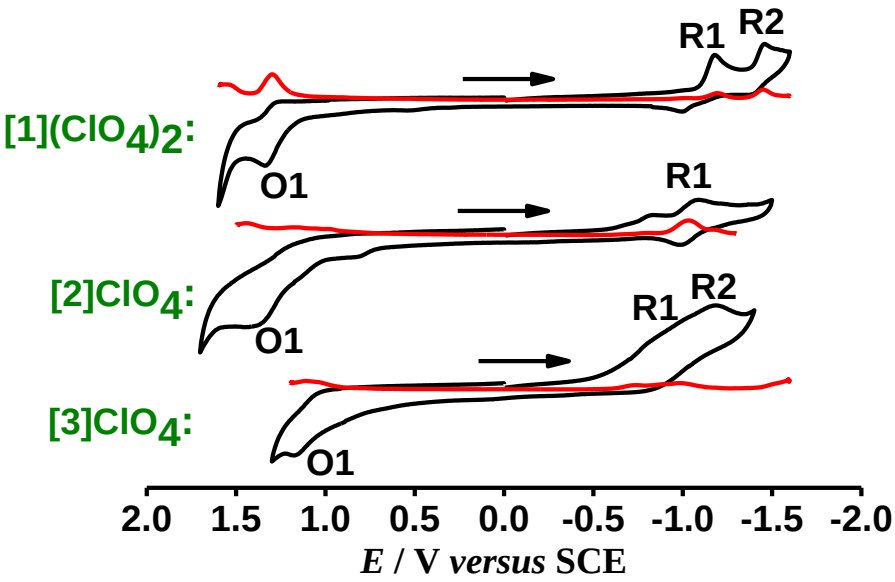

Fig. S10a Cyclic (black) and differential pulse (red) voltammograms in CH_3CN/0.1 MEt_4NClO_4.

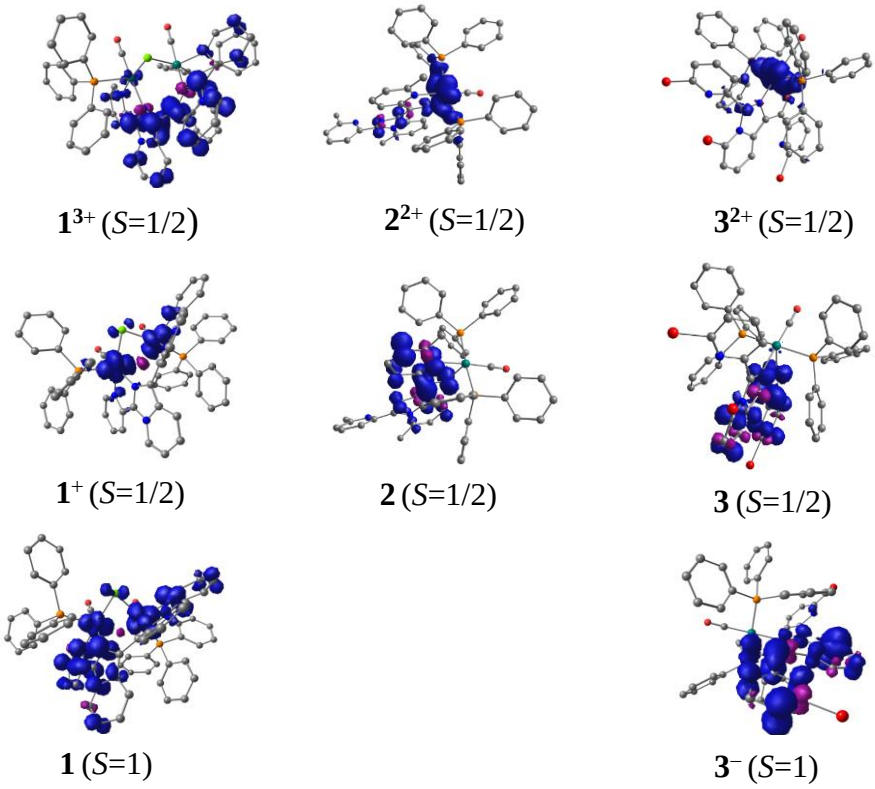

Fig. S10b DFT calculated Mulliken spin density plots (isosurface value 0.002).

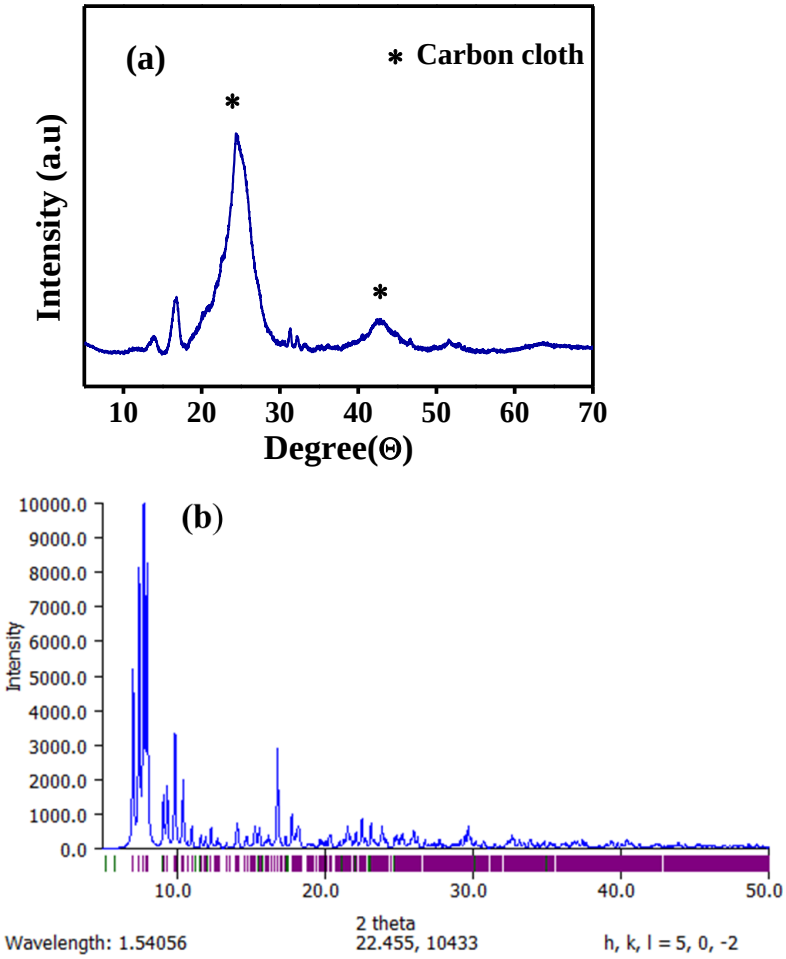

Fig. S11 (a) Powder X-ray diffraction pattern of [**1**]$(ClO_4)_2$ after deposition on CC. (b) PXRD pattern of [**1**]$(ClO_4)_2$ as deduced from the single crystal diffraction data. The peaks at 2Θ values 11, 14 and 17 are in agreement with the simulated PXRD data of molecular complex, implying the retention of molecular structure on carbon cloth support.

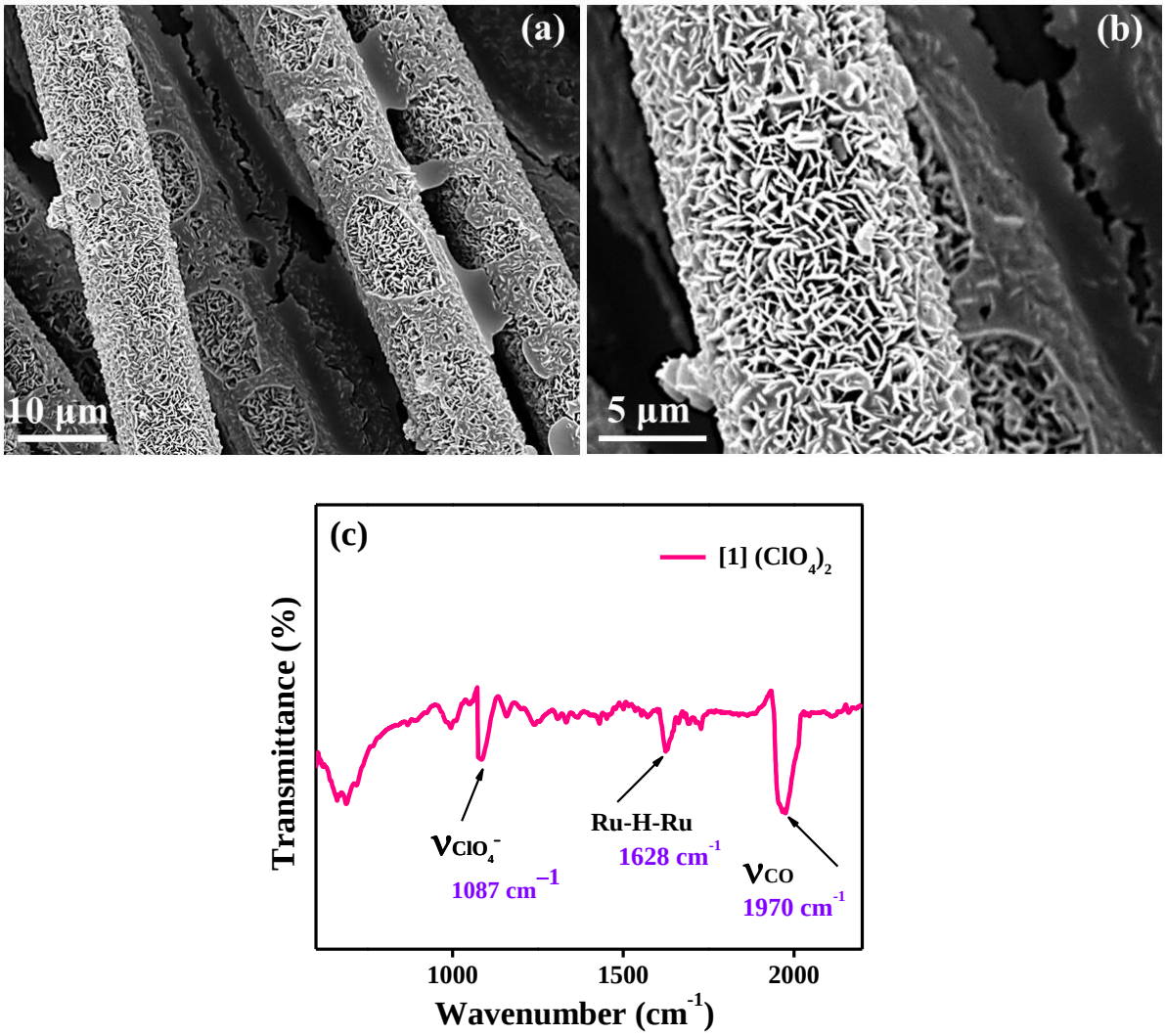

Fig. S12 (a-b) SEM image of [**1**]$(ClO_4)_2$ after deposition on CC showing homogeneous dispersion of catalyst; (c) IR spectrum of [**1**]$(ClO_4)_2$ on CC. Peaks align well with the powder sample, suggesting that the molecular structure remains intact after deposition onto the carbon cloth. The carbonyl and Ru-H-Ru peaks have shifted to negative wavenumbers, indicating interaction between the catalyst and the carbon cloth support.

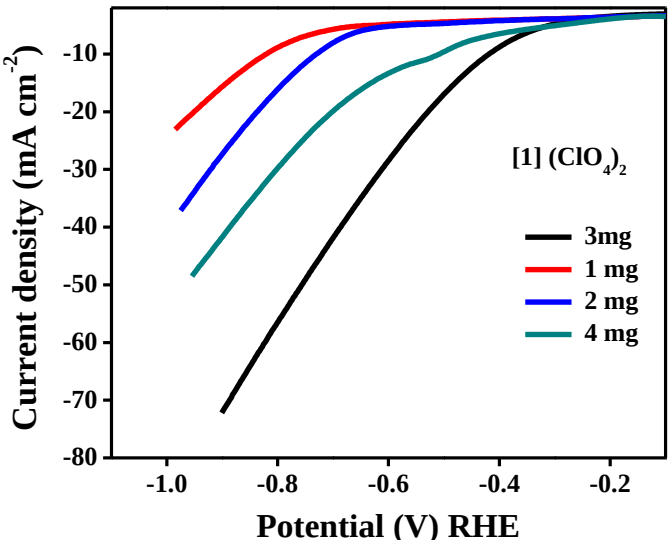

Fig. S13 HER activity of [**1**]$(ClO_4)_2$ with different amount of loading. With increasing amount of catalyst loading (1-4 mg) on CC, the HER activity increases up to 3 mg of loading. After the excess loading, no improvement was observed. In addition, higher loading crosses the limit of carbon cloth to hold the catalyst on it, causing leaching and inhomogeneous distribution of the catalyst on the support. Scan rate: 5 mV s^{-1}.

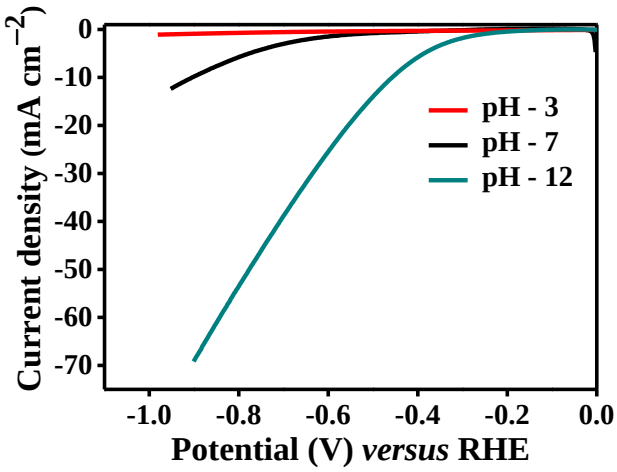

Fig. S14 Linear sweep voltammetric profiles for electrochemical hydrogen evolution with [**1**]$(ClO_4)_2$ at different pH values, showing the best catalytic activity at pH 12. Scan rate: 5 mV s^{-1}.

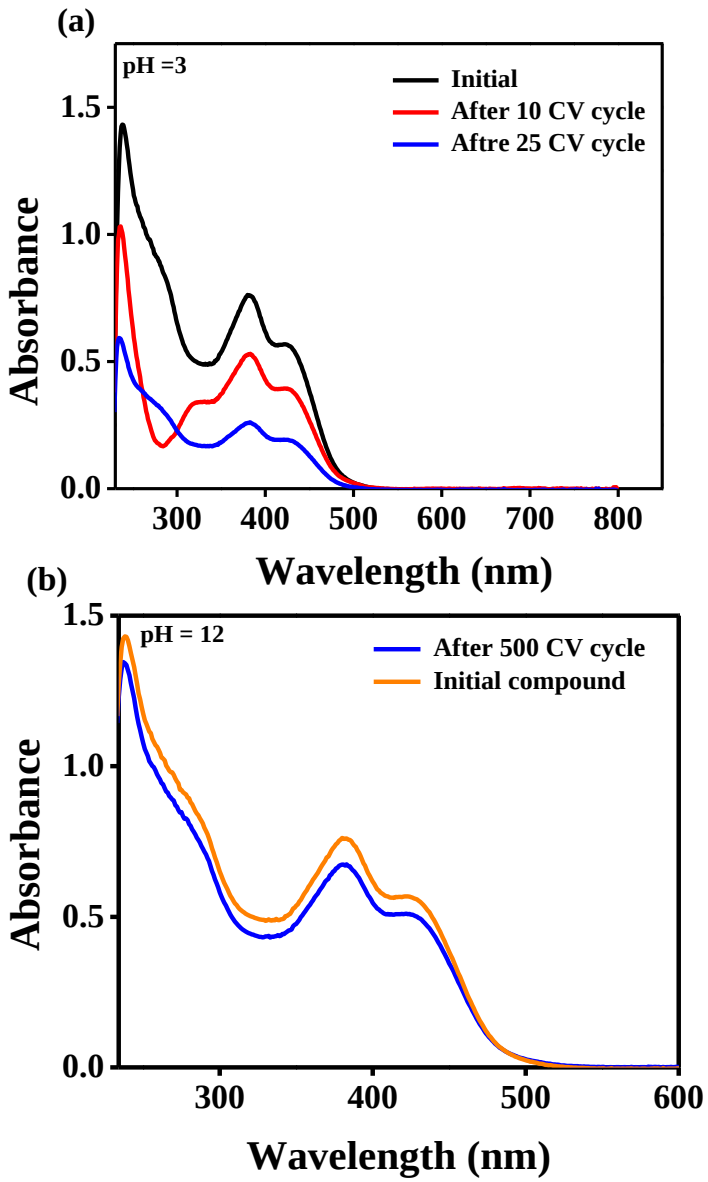

Fig. S15 (a) UV-vis spectra of [**1**]$(ClO_4)_2$ after HER in dichloromethane showing the leaching of catalyst in the acidic medium (pH 3). After 10 CV cycles in the acidic medium, 34% of the catalyst was leached out from the carbon cloth, while the leaching was increased to 67% after 25 CV cycles; (b) UV-vis spectra of [**1**]$(ClO_4)_2$ after 500 CV cycles at pH 12 showing 88% retention of the catalyst.

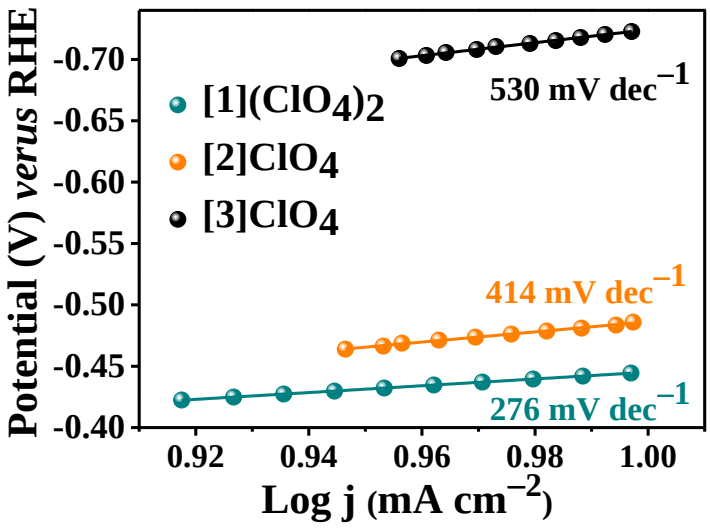

Fig. S16 Tafel analyses of the synthesised complexes under semi-stationary conditions.

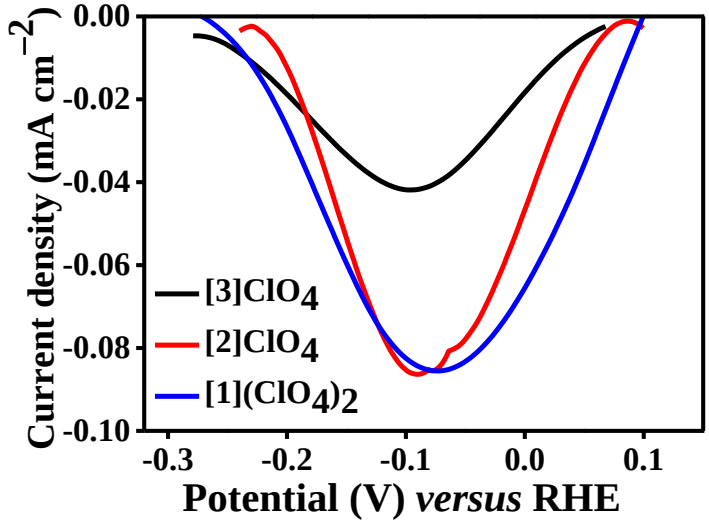

Fig. S17 Reduction peaks for complexes [**1**]$(ClO_4)_2$, [**2**]ClO_4 and [**3**]ClO_4 were utilised to calculate the number of active Ru-sites.

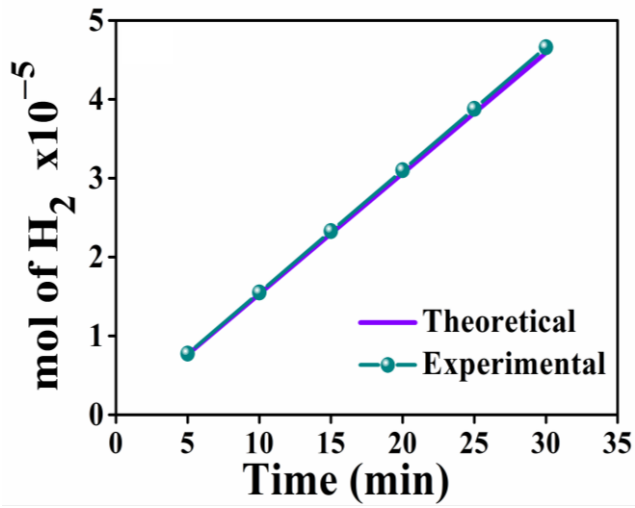

Fig. S18 Faradaic efficiency determined for [**1**]$(ClO_4)_2$ by comparing the amount of hydrogen produced (experimentally) with that of the theoretical values.

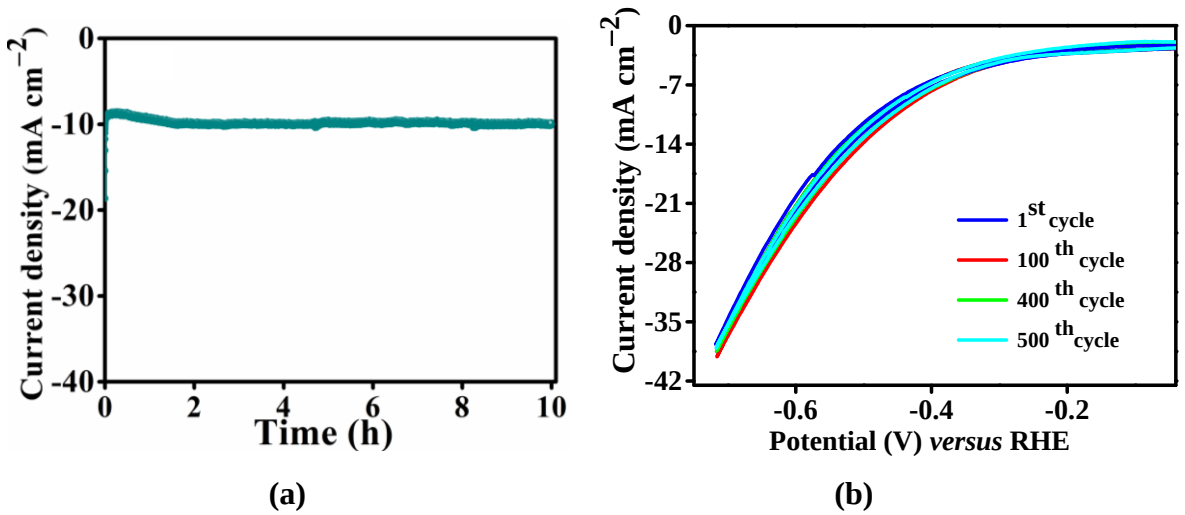

Fig. S19 (a) Chronoamperometric stability test of complex [**1**]$(ClO_4)_2$ over a period of 10 h at -0.45 V vs RHE; (b) Cyclic voltammetric experiments reflecting no significant decrease in activity till 500 CV cycles (Scan rate: 20 mV s^{-1}).

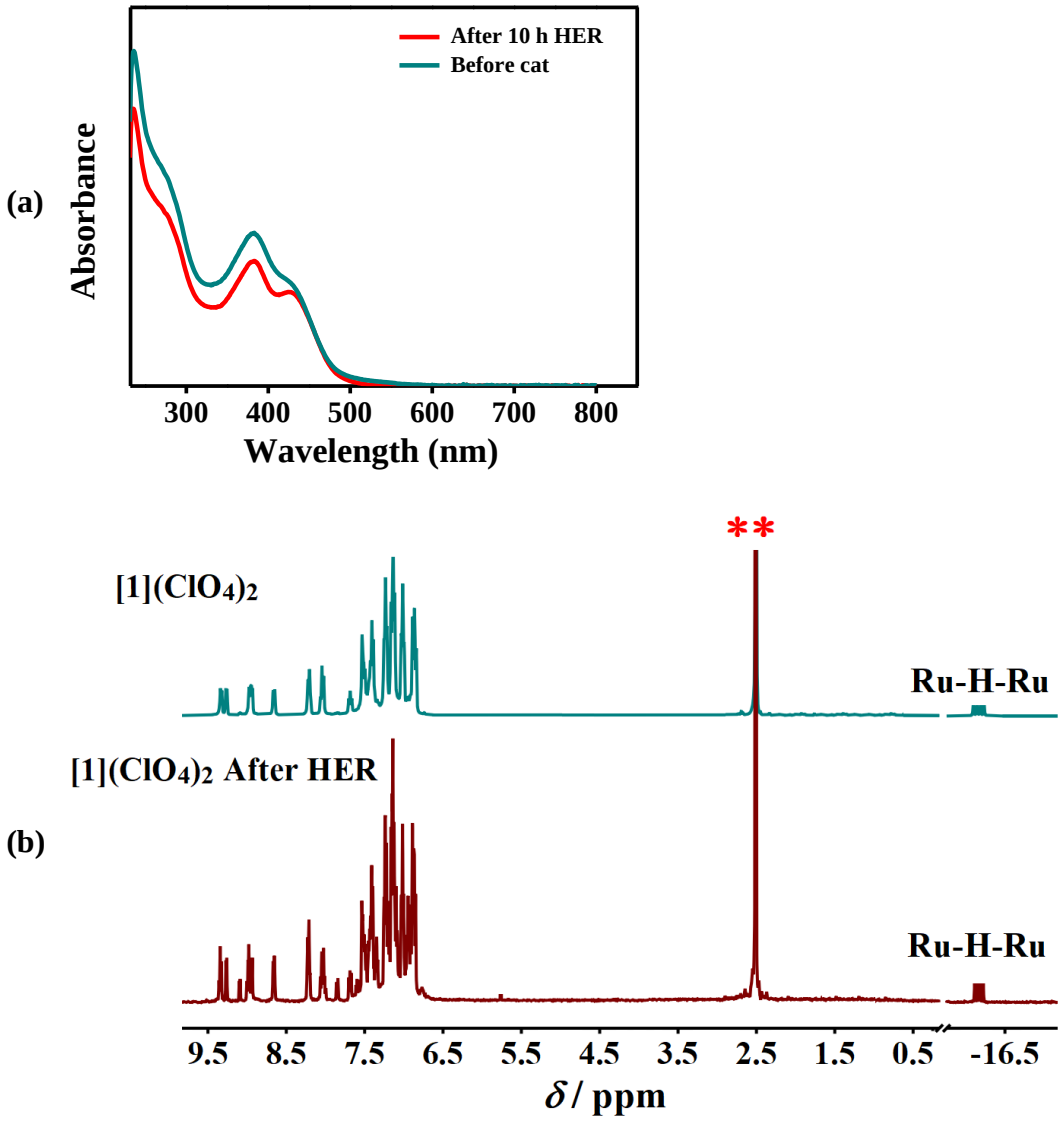

Fig. S20 (a) UV-vis spectra of [**1**]$(ClO_4)_2$ in dichloromethane showing no shift in peak position even after 10 h of CA HER, indicating the retention of the molecular entity after HER. (b) ^{1}H NMR spectra before and after the HER process showing no change of the Ru-H peak position as well as the structure of the catalyst.

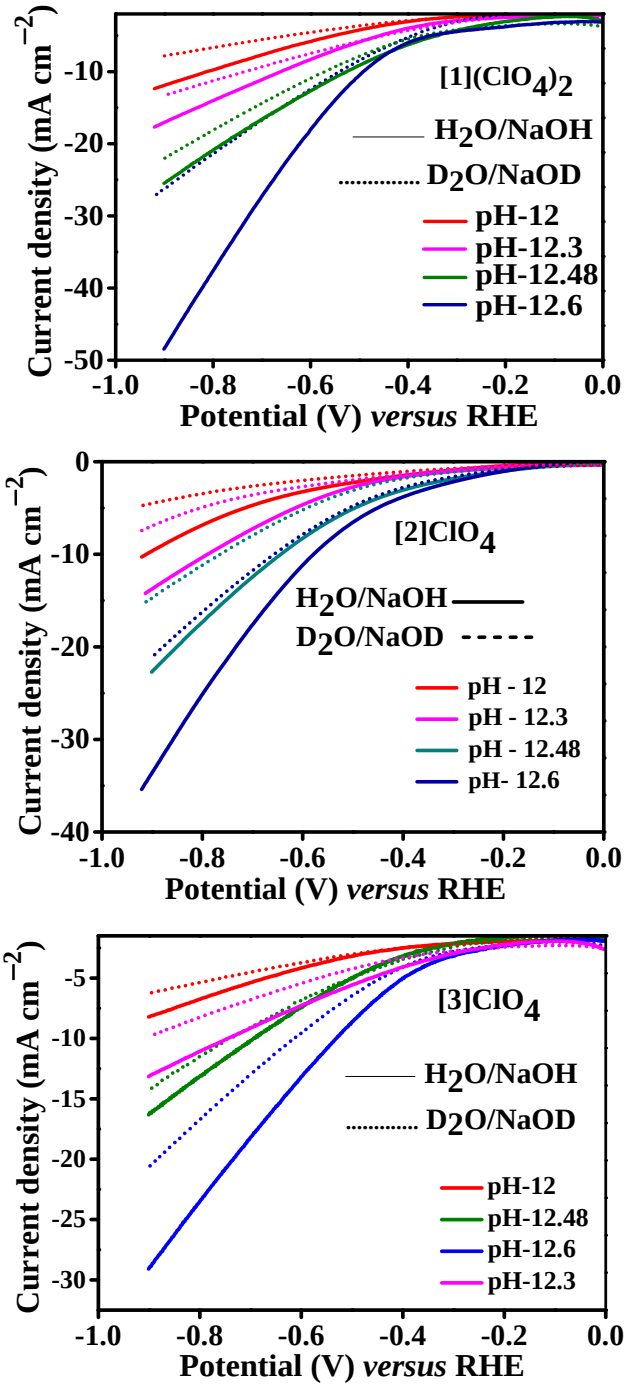

Fig. S21 LSV curves in $NaOH/H_2O$ and $NaOD/D_2O$ at different pHs (Scan rate: 5 mV s^{-1}).

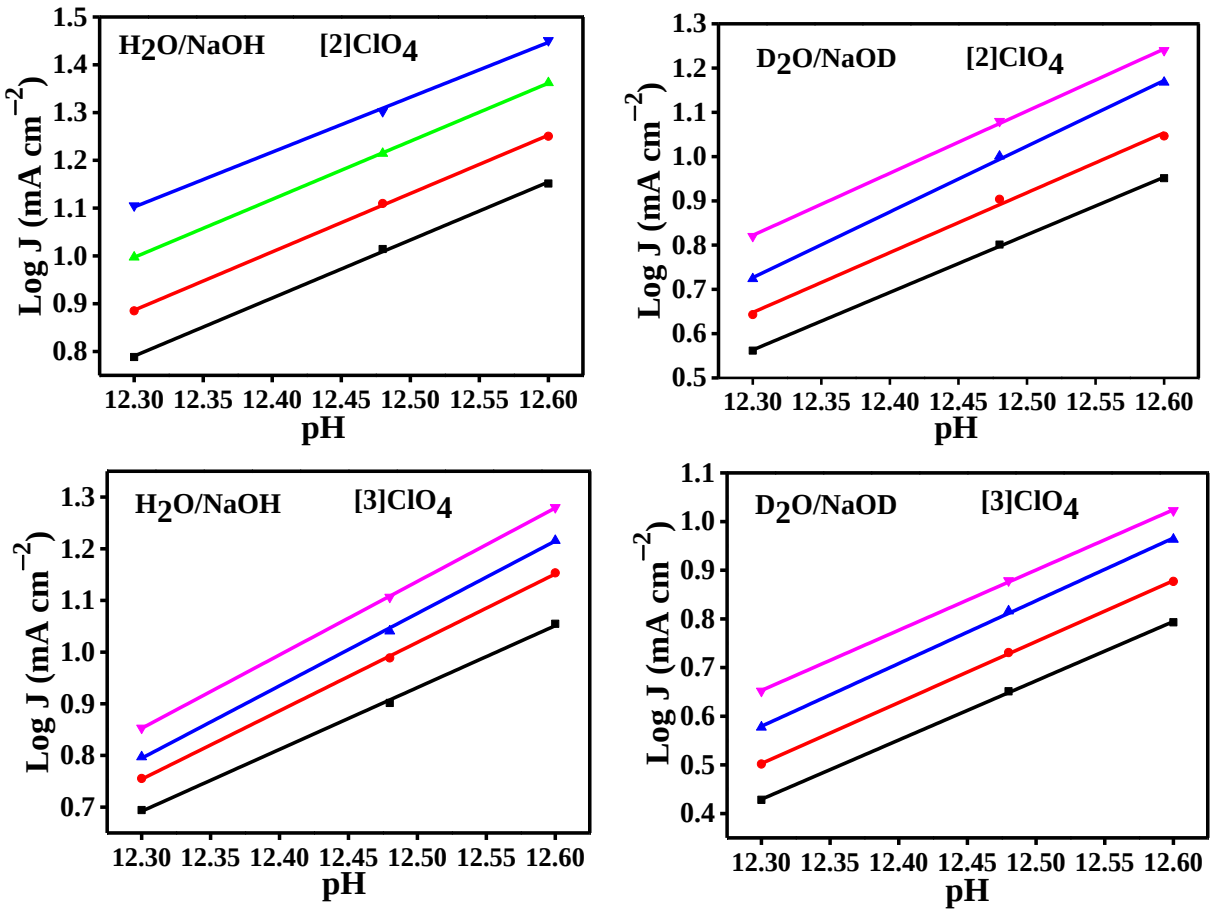

Fig. S22 The pH-dependent kinetic study in H_2O/ NaOH and D_2O/NaOD.

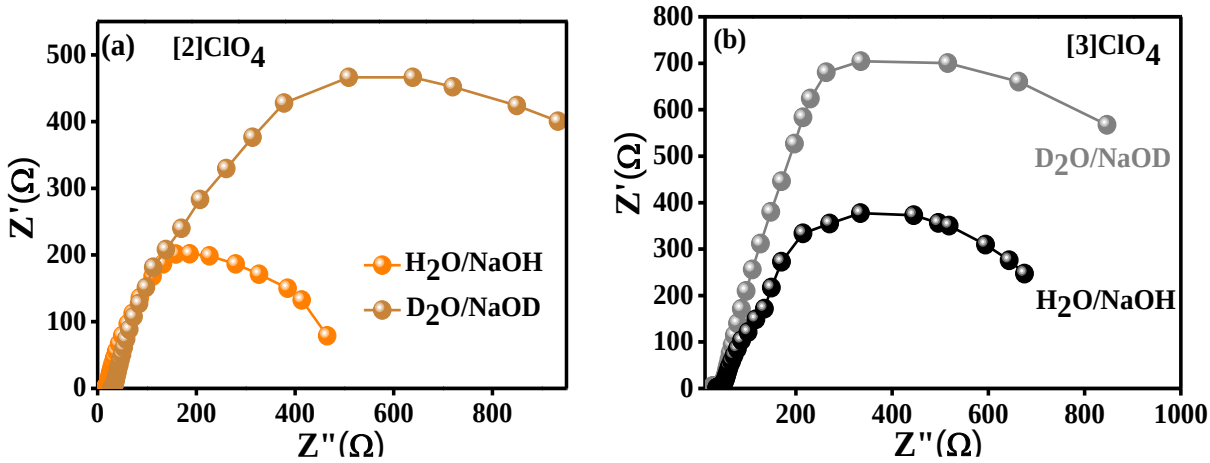

Fig. S23 EIS curves of complexes (a) [**2**]ClO_4 and (b) [**3**]ClO_4 in H_2O/NaOH and D_2O/NaOD.

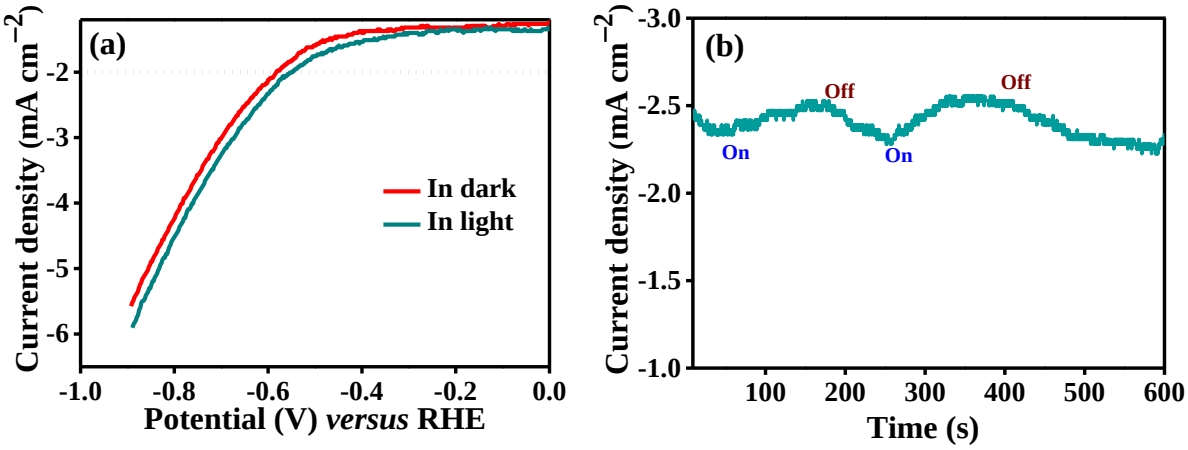

Fig. S24 (a) Linear sweep voltammetric profiles for photoelectrochemical hydrogen evolution with [**1**]$(ClO_4)_2$ (Scan rate: 5 mV s^{-1}) and (b) Photocurrent measurements at chopped light (Potential: -0.38 V vs RHE).

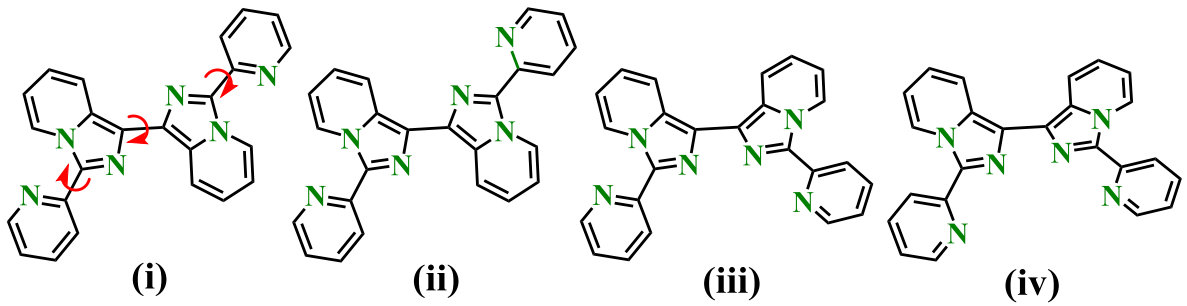

Scheme S1 Varying configuration of L1.

O1: $[(PPh_3)(CO)Ru^{II}(\mu\text{-}H)(\mu\text{-}L1^{\bullet+})(\mu\text{-}Cl)Ru^{II}(CO)(PPh_3)]^{3+}$

$\mathbf{1}^{3+}$ (S=1/2)

$\uparrow -e^-$

Native: $[(PPh_3)(CO)Ru^{II}(\mu\text{-}H)(\mu\text{-}L1)(\mu\text{-}Cl)Ru^{II}(CO)(PPh_3)]^{2+}$

$\mathbf{1}^{2+}$ (S=0)

$\downarrow +e^-$

R1: $[(PPh_3)(CO)Ru^{II}(\mu\text{-}H)(\mu\text{-}L1)(\mu\text{-}Cl)Ru^{I}(CO)(PPh_3)]^{+}$

$\mathbf{1}^{+}$ (S=1/2)

$\downarrow +e^-$

R2: $[(PPh_3)(CO)Ru^{II}(\mu\text{-}H)(\mu\text{-}L1^{\bullet-})(\mu\text{-}Cl)Ru^{I}(CO)(PPh_3)]$

$\mathbf{1}$ (S=1)

Scheme S2 Electronic forms for $\mathbf{1}^n$.

O1: $[(PPh_3)_2(H)(CO)Ru^{III}(L2'/L3')]^{2+}$ / $[(PPh_3)_2(H)(CO)Ru^{II}(L2'^{\bullet+}/L3'^{\bullet+})]^{2+}$

$\mathbf{2}^{2+}$ / $\mathbf{3}^{2+}$ (S=1/2)

$\uparrow -e^-$

Native: $[(PPh_3)_2(H)(CO)Ru^{II}(L2'/L3')]^{+}$

$\mathbf{2}^{+}$ / $\mathbf{3}^{+}$ (S=0)

$\downarrow +e^-$

R1: $[(PPh_3)_2(H)(CO)Ru^{II}(L2'^{\bullet-}/L3'^{\bullet-})]$

$\mathbf{2}$ / $\mathbf{3}$ (S=1/2)

$\downarrow +e^-$

R2: $[(PPh_3)_2(H)(CO)Ru^{II}(L3'^{\bullet 2-})]^{-}$

$\mathbf{3}^{-}$ (S=1)

Scheme S3 Electronic forms for $\mathbf{2}^n$/$\mathbf{3}^n$.

Equation S1:

[**1**]$(ClO_4)_2$**:**

Calculated area associated with the reduction peak = 0.000823×10^{-3} V A

Hence the associated charge was = 0.000823×10^{-3} V A / 0.05 V s^{-1}

= 0.01646×10^{-3} As

= 0.01646×10^{-3} C

Now, the number of electron transferred was = 0.01646×10^{-3} C / 1.602×10^{-19} C

= 10.23×10^{13}

The number of electrons calculated above was the same as the number of the surface active sites due to a single electron transfer involving the Ru^{2+}/Ru^{1+} reduction.

Hence, the surface-active sites that participated in HER = **10.23×10^{13}**

[**2**]ClO_4**:**

Calculated area associated with the reduction peak = 0.000831×10^{-3} V A

Hence the associated charge was = 0.000831×10^{-3} V A / 0.05 V s^{-1}

= 0.01662×10^{-3} As

= 0.01662×10^{-3} C

Now, the number of electron transferred was = 0.01662×10^{-3} C / 1.602×10^{-19} C

= 10.37×10^{13}

The surface-active site that participated in HER = **10.37×10^{13}**

[**3**]ClO_4**:**

Calculated area associated with the reduction peak = 0.000370×10^{-3} V A

Hence the associated charge was = 0.000370×10^{-3} V A / 0.05 V s^{-1}

= 0.0074×10^{-3} As

= 0.0074×10^{-3} C

Now, the number of electron transferred was = 0.0074×10^{-3} C / 1.602×10^{-19} C

$= 4.61 \times 10^{13}$

The surface-active site that participated in HER = **4.61×10^{13}**

Equation S2: Calculation of Turn over frequency (TOF) of different catalysts

$TOF = (j \times N_A) / (2 \times F \times n)$

Where,

j = current density at η = 445 mV

N_A = Avogadro number

F = Faraday constant

n = number of active Ru-sites

TOF calculation at 445 mV *versus* RHE

[**1**]$(ClO_4)_2$**:**

$TOF = [(10 \times 10^{-3}) (6.023 \times 10^{23})] / [(96485) (2) (10.23 \times 10^{13})]$

TOF = 305.1 s^{-1}

[**2**]ClO_4**:**

$TOF = [(7.99 \times 10^{-3}) (6.023 \times 10^{23})] / [(96485) (2) (10.37 \times 10^{13})]$

TOF = 252.9 s^{-1}

[**3**]ClO_4**:**

$TOF = [(3.66 \times 10^{-3}) (6.023 \times 10^{23})] / [(96485) (2) (4.61 \times 10^{13})]$

TOF = 110.1 s^{-1}

Equation S3:

Calculation of Turn-Over Number (TON) for [1]$(ClO_4)_2$ after 30 minutes HER

TON = moles of produced H_2 / Moles of active Ru-sites

= 4.66×10^{-5} mole of H_2 / (10.23×10^{13} / 6.023×10^{23}) mole active Ru-sites

= **2.74×10^5**

Equation S4:

Determination of the faradaic efficiency of complex [**1**]$(ClO_4)_2$

We have utilised the water displacement method to detect the amount of generated hydrogen. Two-compartment membrane-separated H-cell have been employed to determine the generated hydrogen. We have employed a cathodic current density of –5 mA cm^{-2} for 1800 s. In the first step, we calculated the theoretically generated hydrogen gas using the following equation from Faraday's law. The amount of H_2 generated was determined by following the equation S4.1:

$$nH_2\,(\text{theoretical}) = \frac{Q}{n \times F} = \frac{I \times t}{n \times F} = \frac{0.005 \times 1800\ \text{s}}{2 \times 96485.3\ \text{s A mol}^{-1}} = 0.0000466 \qquad \textbf{(S4.1)}$$

Where nH_2, Q, n, F, I and t represented theoretically calculated amount of H_2, amount of applied charge, number of electrons transferred in HER (2 electrons), Faraday constant (96485.3 s A mol^{-1}), applied current (0.005 A) and reaction time (1800 s), respectively.

After theoretical calculations, the amount of generated hydrogen in mmol at the time of chronoamperometric measurements was measured. Experimentally measured and theoretically calculated amount of hydrogen was then compared to determine the Faradaic efficiency using the following equation S4.2:

$$\text{Faradaic efficiency (\%)} = \frac{nH_2\,(\text{experimental})}{nH_2\,(\text{Theoretical})} \times 100 = \frac{0.0000459}{0.0000466} \times 100 = 98.4\% \qquad \textbf{(S4.2)}$$

A link of short video showing the vigorous hydrogen evolution at the cathode:

https://drive.google.com/file/d/10gamCo61vyuTWjAkpeg3wE9FMKqKw5nP/view?usp=sharing

Table S1 Selected crystallographic parameter

Complex	L3	[**1**]$(ClO_4)_2$	[**2**]ClO_4	[**3**]ClO_4
empirical formula	$C_{24}H_{12}Br_4N_6$	$C_{62}H_{47}Cl_3N_6O_{10}P_2Ru_2$	$C_{58}H_{49}ClN_4O_6P_2Ru$	$C_{56}H_{41}Br_3Cl_4N_4O_6P_2Ru$
formula weight	704.04	1406.48	1096.47	1410.47
crystal system	monoclinic	monoclinic	triclinic	monoclinic
space group	*-I 2ya*	*-P 2ybc*	*P-1*	*-P 2ybc*
a (Å)	11.9288(5)	19.7908(5)	15.6010(2)	18.3915(2)
b (Å)	6.8445(3)	15.1911(4)	21.1050(3)	14.4654(2)
c (Å)	27.4989(11)	23.1446(8)	22.1703(3)	20.9301(3)
α (deg)	90	90	110.1520(10)	90
β (deg)	90.376(4)	107.604(3)	101.1340(10)	100.8040(10)
γ (deg)	90	90	99.6610(10)	90
V (Å^3)	2245.15(16)	6632.4(3)	6502.66(16)	5469.55(13)
Z	4	4	4	4
μ (mm^{-1})	7.198	0.683	0.376	2.787
T (K)	109.5(7)	150.00(10)	150.00(10)	150.00(10)
Dcalcd (g cm^{-3})	2.083	1.409	1.120	1.713
F (000)	1352.0	2840.0	2256	2800.0
θ range(deg)	5.926-49.99	1.6390-19.6720	1.784-23.889	1.747-29.618
data/restraints/ parameters	1984/0/154	11661/26/788	22925/0/1306	9625/0/689
R1, wR2 [I>2σ(I)]	0.0637, 0.1541	0.0583, 0.128	0.0772, 0.1433	0.0392, 0.0831
R1, wR2(all data)	0.1031, 0.1786	0.1132, 0.1515	0.0545, 0.1610	0.0330, 0.0869
GOF	1.011	1.028	1.032	1.014
largest diff. peak/hole [e Å^{-3}]	2.59/–0.91	0.687/–0.689	0.930/–0.777	0.971/–1.169

Table S2 Selected experimental and DFT calculated bond lengths (Å)

Bond lengths (Å)	[**1**]$(ClO_4)_2$		[**2**]ClO_4		[**3**]ClO_4	
	X-ray	DFT	X-ray	DFT	X-ray	DFT
Ru1-N1	2.119(4)	2.172	2.171(3)	2.243	2.148(3)	2.191
Ru1-N2	2.142(4)	2.210	-	-	-	-
Ru2-N5	2.064(4)	2.194	-	-	-	-
Ru2-N4	2.121(4)	2.121	-	-	-	-
Ru1-C61	1.832(6)	1.868	-	-	-	-
Ru2-C60	1.839(7)	1.873	-	-	-	-
Ru1-P1	2.2713(16)	2.444	2.3612(10)	2.446	2.3520(8)	2.451
Ru1-P2	-	-	2.3543(10)	2.447	2.3670(8)	2.447
Ru2-P2	2.3249(16)	2.379	-	-	-	-
Ru1-H	1.66(5)	1.860	1.72(3)	1.59	1.62(3)	1.587
Ru2-H	1.85(5)	1.744	-	-	-	-
Ru1-Cl1	2.4353(16)	2.489	-	-	-	-
Ru2-Cl1	2.3846(15)	2.534	-	-	-	-
C5-N1	1.368(7)	1.361	-	-	-	-
C6-N2	1.329(6)	1.366	-	-	-	-
C19-N4	1.338(7)	1.344	-	-	-	-
C20-N5	1.346(7)	-	-	-	-	-
C5-C6	1.426(7)	1.369	-	-	-	-
C12-C13	1.434(7)	1.450	-	-	-	-
C19-C20	1.439(7)	1.454	-	-	-	-
Ru1-Ru2	2.8588(6)	3.034	-	-	-	-
Ru1-O1	-	-	2.151(2)	2.230	2.208(2)	2.262
Ru1-C54	-	-	1.853(5)	1.861		
Ru1-C55	-	-	-	-	1.836(3)	1.8675
C1-O1	-	-	1.253(4)	1.256	1.254(4)	1.256
C61-O1	1.139(6)	1.154	-	-	-	-
C60-O2	1.139(6)	1.154	-	-	-	-
C58-O2	-	-	1.127(5)	1.160	-	-
C55-O2			-	-	1.164(4)	1.158
C2-N1	-	-	1.376(4)	1.368	1.381(4)	1.387
C15-C16	-	-	1.481(5)	1.501	1.481(5)	1.415
C1-C2	-	-	1.497(5)	1.503	1.494(4)	1.484
Ru2-O7			2.147(3)	2.148		
Ru2-N5			2.174(3)	2.168		

Table S3a Selected experimental and DFT calculated bond lengths (Å)

Bond lenghths (Å)	L3	
	X-ray	DFT
N1-C7	1.332(12)	1.329
N1-C1	1.357(11)	1.357
N2-C12	1.296(11)	1.315
N3-C2	1.416(11)	1.421
C9-C8	1.402(13)	1.402
C9-C10	1.369(13)	1.409
C7-C8	1.490(12)	1.468

Table S3b Selected experimental and DFT calculated bond angles (deg)

Bond Angles (deg)	L3	
	X-ray	DFT
N1-C1-C2	111.5(8)	109.7
C1-C2-C3	136.3(8)	134.4
N1-C7-N3	136.3(8)	134.8
C8-C7-N1	122.0(9)	1.421
C4-C3-C2	120.3(9)	122.7

Table S4 Selected experimental and DFT calculated bond angles (deg)

Bond angles (deg)	[**1**]$(ClO_4)_2$		[**2**]ClO_4		[**3**]ClO_4	
	X-ray	DFT	X-ray	DFT	X-ray	DFT
N1-Ru1-N2	76.39(17)	76.14	-	-	-	-
N2-Ru1-P1	95.60(12)	90.74	-	-	-	-
Cl1-Ru1-H	90.7(17)	84.99	-	-	-	-
P2-Ru1-Ru1	115.79(4)	117.88	-	-	-	-
Ru1-Cl1-Ru2	52.81(4)	74.31	-	-	-	-
Ru1-H-Ru2	37.9(17)	114.58	-	-	-	-
N4-Ru2-N5	76.86(17)	75.83	-	-	-	-
N5-Ru2-P2	90.45(12)	94.96	-	-	-	-
Cl1-Ru2-H	87.9(15)	86.02	-	-	-	-
N1-Ru1-O1	2.119(4)	-	73.64(8)	73.02	74.76(8)	72.00
P2-Ru1-O1	2.142(4)	-	92.51(5)	93.42	92.26(6)	90.57
P1-Ru1-N1	2.064(4)	-	90.94(5)	91.49	92.79(6)	91.63
P2-Ru1-P1	2.121(4)	-	176.54(3)	171.63	174.92(3)	177.1
H-Ru1-O1	1.368(7)	-	172.9(10)	170.72	170.0(10)	167.58
C54-Ru1-N1	1.329(6)	-	178.49(11)	174.89	-	-
C55-Ru1-N1	-	-	-	-	174.71(11)	179.21

Table S5 Energies of DFT ((U)/(R)B3LYP/LanL2DZ/6-31G*) optimised structures

Complex	*E* (Hartrees)		$\Delta E_{(HE-LE)}$[a]
	S = 0	*S* = 1	
1	-4200.6441727	**-4200.6481401**	0.0039674 Hartrees 870.74364706 cm^{-1} 10.416409493 kJ/mol
2⁻	-10980.2606765	**-10980.2700783**	0.0094018 Hartrees 2063.456576334 cm^{-1} 24.68442778036 kJ/mol

[a]HE = Spin state in higher in energy and LE = Spin state in lower in energy.

Table S6 π---π interaction in (Å)

Interaction π---π (Å)	[**1**]$(ClO_4)_2$	[**2**]ClO_4	[**3**]ClO_4
C60---C56	3.534	-	-
C37---C56	3.552		
C7---O6	3.191	-	-
C11---O6	3.085	-	-
C39---O4	3.327	-	
C24---O7	3.391	-	-
C23---O8	3.318	-	-
C12---C37		3.499	
C11---C37	-	3.499	-
C4···O6	-	3.169	-
C47---O5		3.386	
C41---C13	-	-	3.487
C39---C52	-	-	3.513
C53---C46	-	-	3.472
C5---O5	-	-	3.285
C6---O5	-	-	3.178

Table S7 Experimental and TD-DFT (B3LYP/6-31G*/LANL2DZ) calculated electronic transitions.

λ_{max}/nm (expt.)[a] (ε/dm^{3}mol^{-1}cm^{-1})[b]	λ/nm (DFT) (f)[c]	Transitions	Character
1^{2+} (S=0)			
429 (39000)	412 (0.09)	HOMO-3→LUMO+2(0.34)	Ru(dπ)/PPh$_3$(π)→L1(π*)
380 (59000)	385 (0.02)	HOMO-2→LUMO(0.34)	Ru(dπ)/PPh$_3$(π)→L1(π*)
	369 (0.60)	HOMO→LUMO+3(0.65)	L1(π)→L1(π*)/Ru(dπ)
267 (93000)	305 (0.02)	HOMO-8→LUMO(0.42)	Ru(dπ)→L1(π*)
	301 (0.01)	HOMO-1→LUMO+3(0.46)	Ru(dπ)/PPh$_3$(π)→L1(π*)
2^{+} (S=0)			
475 (23000)	478 (0.30)	HOMO→LUMO(0.67)	L2′(π)/Ru(dπ)→L2′(π*)
399 (18000)	389 (0.20)	HOMO→LUMO+1(0.58)	L2′(π)/Ru(dπ)→L2′(π*)
275 (51000)	283 (0.01)	HOMO-2→LUMO+3(0.14)	Ru(dπ)→L2′(π*)
3^{+} (S=0)			
419 (30000)	414 (0.01)	HOMO-2→LUMO(0.64)	Ru(dπ)/L3′(π)→L3′(π*)
	391 (0.10)	HOMO-1→LUMO(0.52)	Ru(dπ)/PPh$_3$(π)→L3′(π*)
325 (31000)	329 (0.08)	HOMO→LUMO+1(0.48)	PPh$_3$(π)/L3′(π)→L3′(π*)

[a]Experimental absorption maxima from spectroelectrochemistry in CH_3CN/0.1 M Et_4NClO_4.

[b]Molar extinction coefficients in dm^{3}mol^{-1}cm^{-1}. [c]Calculated oscillator strengths.

Table S8 Electrochemical data[a]

Complex	E°_{298}/[V](ΔE_p/[mV])[b]		
	O1	R1	R2
[1]$(ClO_4)_2$	1.31[c]	−1.09[c]	−1.40[c]
[2]ClO_4	1.26[c]	−1.03[c]	-
[3]ClO_4	1.05[c]	−0.78[c]	−1.07[c]

[a]From cyclic voltammetry in CH_3CN/0.1 M Et_4NClO_4 at 100 mVs^{-1}. [b]Peak potentials in V versus SCE.[c]Irreversible.

Table S9 DFT calculated MO compositions for **1**$^{3+}$ in S = 1/2 state

MO	Energy (eV)	% Composition					
		Ru	L1	PPh_3	CO	Cl	H
			α-MO				
LUMO+5	-8.373	17	61	18	01	03	00
LUMO+4	-8.517	27	46	23	01	04	00
LUMO+3	-9.108	02	94	03	00	00	00
LUMO+2	-9.249	02	95	02	00	00	00
LUMO+1	-9.345	08	85	03	01	03	00
LUMO	-9.481	06	89	04	01	00	01
SOMO	-12.775	03	01	96	00	00	00
HOMO-1	-12.920	56	06	34	01	03	00
HOMO-2	-13.027	26	05	63	00	05	00
HOMO-3	-13.068	07	03	87	00	03	00
HOMO-4	-13.142	03	59	37	01	00	00
HOMO-5	-13.171	06	02	92	02	00	00
			β-MO				
LUMO+5	-8.477	28	42	25	01	05	00
LUMO+4	-8.968	02	94	04	00	00	00
LUMO+3	-9.078	02	95	03	00	00	00
LUMO+2	-9.225	09	83	04	01	03	00
LUMO+1	-9.376	06	88	04	01	00	01
LUMO	-12.181	03	83	12	00	01	00
HOMO	-12.567	01	14	85	00	00	00
HOMO-1	-12.900	62	07	28	01	02	01
HOMO-2	-13.015	23	04	66	00	06	00
HOMO-3	-13.058	06	04	88	00	02	00
HOMO-4	-13.156	06	02	92	00	00	00
HOMO-5	-13.169	12	12	72	00	03	00

α-MO			
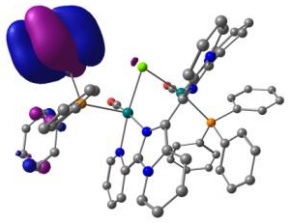	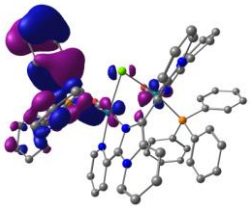	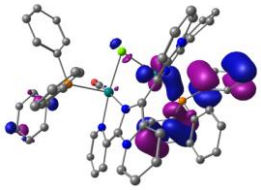	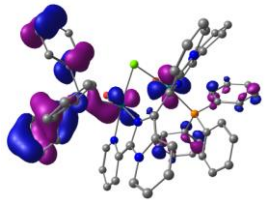
SOMO	HOMO-1	HOMO-2	HOMO-3
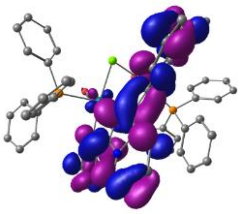	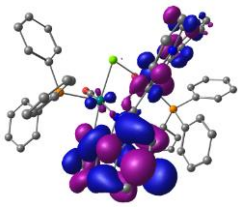	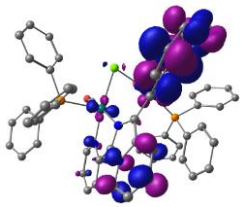	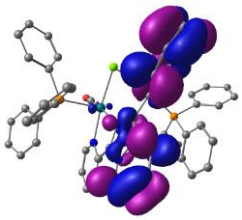
LUMO	LUMO+1	LUMO+2	LUMO+3
β-MO			
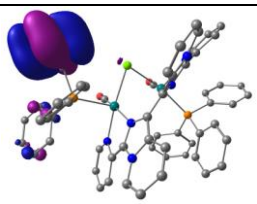	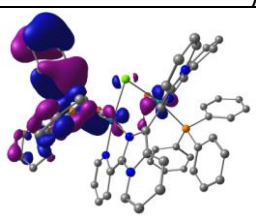	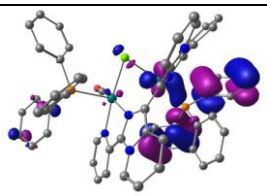	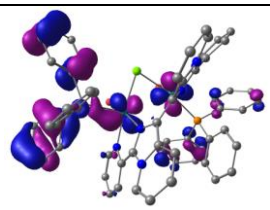
HOMO	HOMO-1	HOMO-2	HOMO-3
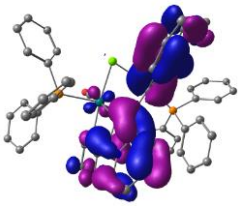	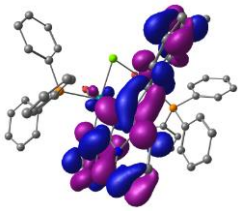	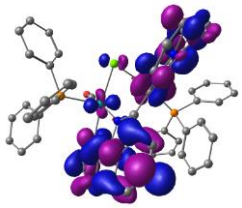	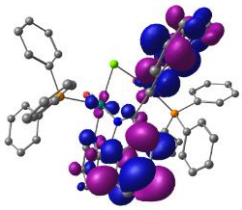
LUMO	LUMO+1	LUMO+2	LUMO+3

Table S10 DFT calculated MO compositions for **1**$^{2+}$ in S = 0 state

MO	Energy (eV)	% Composition					
		Ru	L1	PPh_3	CO	Cl	H
LUMO+5	-5.664	04	91	05	01	00	00
LUMO+4	-5.976	08	84	07	00	01	00
LUMO+3	-6.145	20	64	13	00	03	00
LUMO+2	-6.242	12	79	07	01	01	00
LUMO+1	-6.503	24	58	11	01	05	00
LUMO	-6.548	14	80	03	02	01	01
HOMO	-9.726	02	97	01	00	00	00
HOMO-1	-10.285	35	04	59	00	01	00
HOMO-2	-10.334	52	06	40	00	02	00
HOMO-3	-10.496	22	05	64	00	08	00
HOMO-4	-10.590	07	04	87	01	00	00
HOMO-5	-10.666	20	28	44	02	06	01

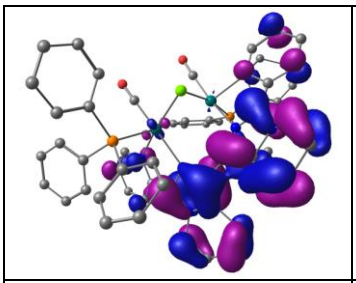	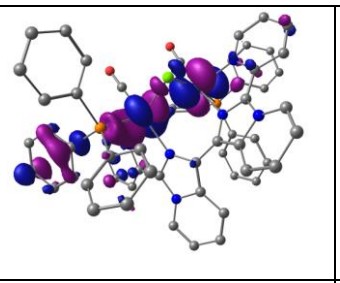	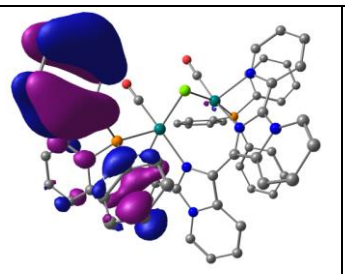	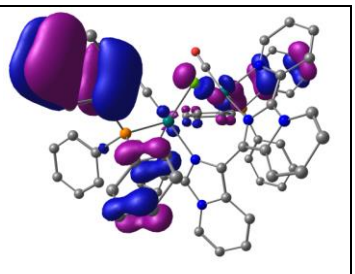
HOMO	HOMO-1	HOMO-2	HOMO-3
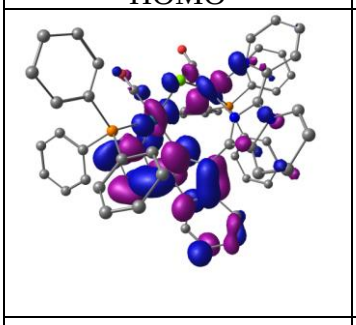	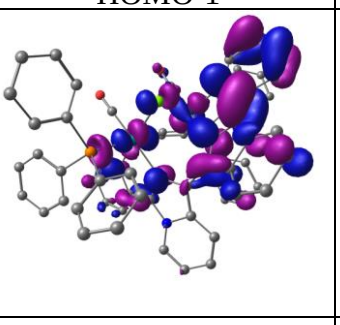	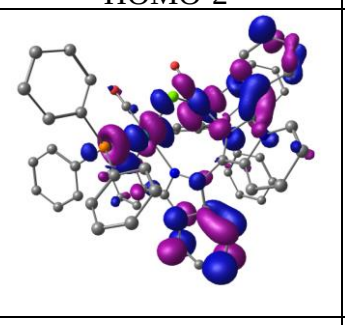	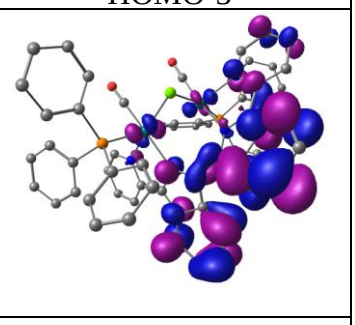
LUMO	LUMO+1	LUMO+2	LUMO+3

Table S11 DFT calculated MO compositions for **1**$^{+}$ in S = 1/2 state

MO	Energy (eV)	% Composition					
		Ru	L1	PPh_3	CO	Cl	H
			α-MO				
LUMO+5	-3.065	07	80	11	01	01	00
LUMO+4	-3.213	15	64	16	01	04	00
LUMO+3	-3.624	04	91	05	00	00	00
LUMO+2	-3.746	02	97	01	00	00	00
LUMO+1	-3.842	14	72	12	00	01	00
LUMO	-4.039	08	85	05	01	01	01
SOMO	-5.127	47	28	17	02	06	00
HOMO-1	-7.403	70	21	05	00	03	00
HOMO-2	-7.549	21	75	03	00	01	00
HOMO-3	-7.954	58	11	12	02	17	00
HOMO-4	-8.023	54	11	07	05	21	01
HOMO-5	-8.136	75	07	06	02	10	00
			β-MO				
LUMO+5	-3.099	15	74	09	01	01	00
LUMO+4	-3.305	31	34	30	01	04	00
LUMO+3	-3.640	03	94	02	01	00	00
LUMO+2	-3.723	02	97	01	00	00	00
LUMO+1	-3.915	06	88	03	01	00	01
LUMO	-3.954	10	84	03	01	02	00
HOMO	-7.292	74	17	06	00	03	00
HOMO-1	-7.497	18	78	02	00	01	00
HOMO-2	-7.820	61	12	08	03	16	00
HOMO-3	-7.916	57	12	06	06	19	00
HOMO-4	-8.005	78	06	04	11	01	00
HOMO-5	-8.198	34	44	12	05	05	01

α-MO			
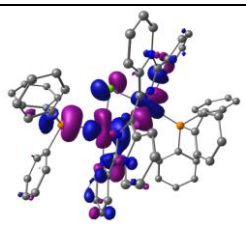	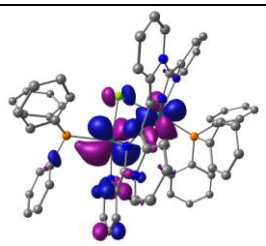	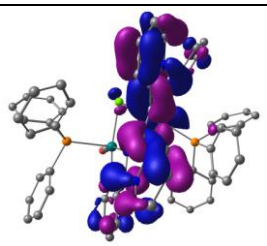	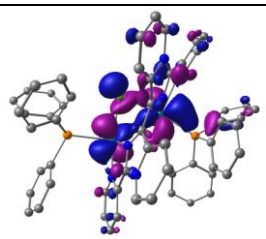
SOMO	HOMO-1	HOMO-2	HOMO-3
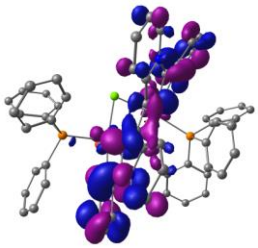	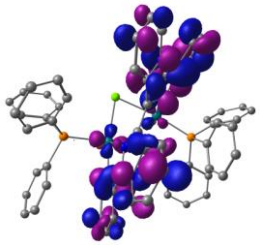	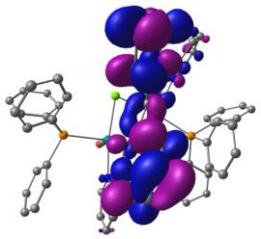	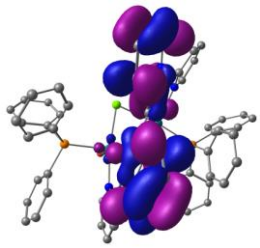
LUMO	LUMO+1	LUMO+2	LUMO+3
β-MO			
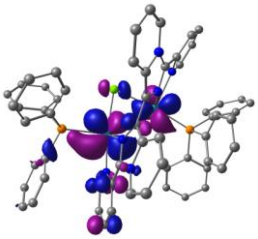	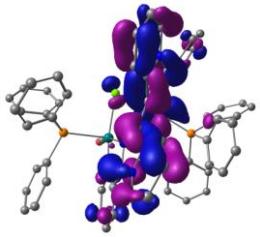	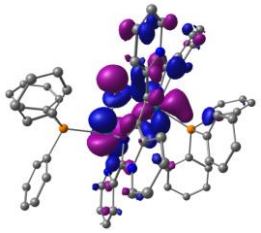	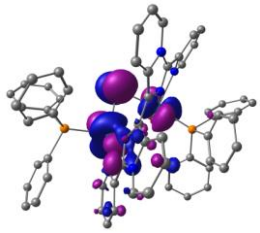
HOMO	HOMO-1	HOMO-2	HOMO-3
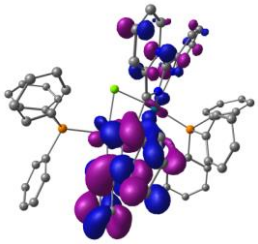	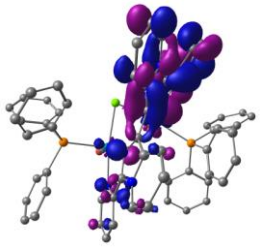	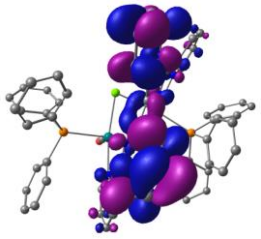	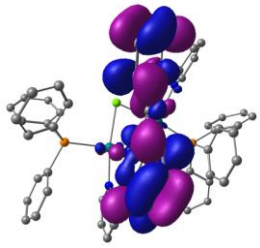
LUMO	LUMO+1	LUMO+2	LUMO+3

Table S12 DFT calculated MO compositions for **1** in *S* = 1 state

MO	Energy (eV)	% Composition					
		Ru	L1	PPh_3	CO	Cl	H
			α-MO				
LUMO+5	-0.309	06	03	89	02	00	00
LUMO+4	-0.369	02	06	90	01	00	00
LUMO+3	-0.445	35	10	53	01	01	00
LUMO+2	-0.750	12	67	20	00	01	00
LUMO+1	-0.900	27	29	39	01	04	00
LUMO	-0.934	02	93	04	01	00	00
SOMO	-1.948	14	70	10	01	04	00
HOMO-1	-2.007	10	82	06	01	01	01
HOMO-2	-4.584	02	95	03	00	01	00
HOMO-3	-5.054	74	14	09	01	03	00
HOMO-4	-5.378	26	56	08	02	08	00
HOMO-5	-5.545	46	22	02	05	25	00
			β-MO				
LUMO+5	-0.359	03	06	90	01	00	00
LUMO+4	-0.507	24	44	31	01	00	00
LUMO+3	-0.573	16	45	37	02	00	00
LUMO+2	-0.678	09	73	16	00	01	00
LUMO+1	-0.844	31	24	36	02	07	00
LUMO	-0.861	03	91	05	01	01	00
HOMO	-4.364	01	96	03	00	00	00
HOMO-1	-4.935	67	22	08	01	02	00
HOMO-2	-5.198	25	64	08	01	02	01
HOMO-3	-5.474	51	13	04	05	27	00
HOMO-4	-5.574	52	16	10	02	20	00
HOMO-5	-5.666	75	09	05	11	20	00

α-MO			
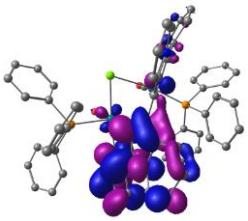	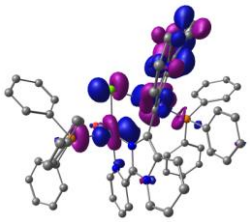	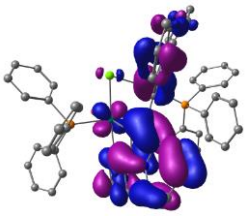	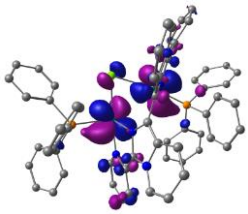
SOMO	HOMO-1	HOMO-2	HOMO-3
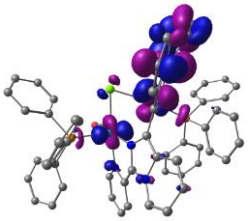	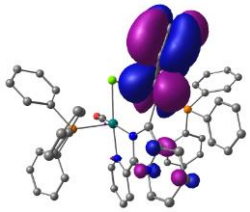	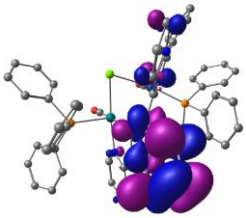	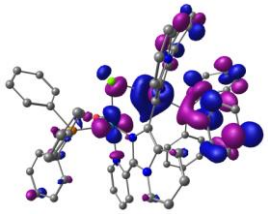
LUMO	LUMO+1	LUMO+2	LUMO+3
β-MO			
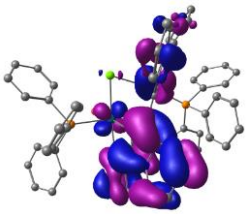	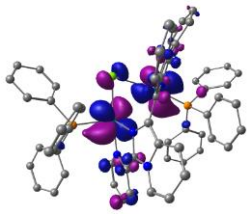	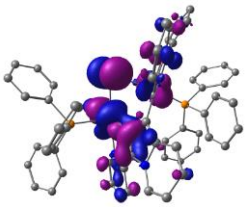	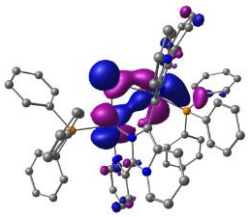
HOMO	HOMO-1	HOMO-2	HOMO-3
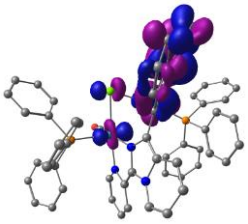	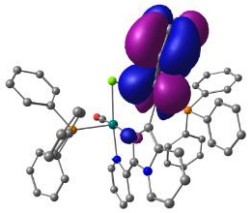	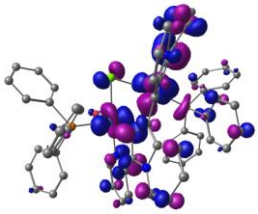	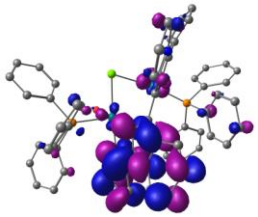
LUMO	LUMO+1	LUMO+2	LUMO+3

Table S13 DFT-calculated MO compositions for $\mathbf{2}^{2+}$ in S = 1/2 state

MO	Energy (eV)	% Composition				
		Ru	L2′	PPh_3	CO	H
			α-MO			
LUMO+5	-5.734	05	86	07	01	00
LUMO+4	-5.816	06	77	16	01	00
LUMO+3	-5.816	06	77	16	01	00
LUMO+2	-5.861	30	11	55	01	02
LUMO+1	-6.279	02	95	03	01	00
LUMO	-7.594	04	89	07	00	00
SOMO	-10.790	00	01	99	00	00
HOMO-1	-10.833	07	17	76	00	00
HOMO-2	-10.955	01	08	91	00	00
HOMO-3	-10.993	03	59	38	00	00
HOMO-4	-11.055	02	09	88	01	00
HOMO-5	-11.166	01	07	92	00	00
			β-MO			
LUMO+5	-5.667	03	91	06	00	00
LUMO+4	-5.768	30	10	58	01	02
LUMO+3	-5.801	03	87	08	01	00
LUMO+2	-6.188	02	95	03	01	00
LUMO+1	-7.498	07	84	10	00	00
LUMO	-9.585	45	33	21	00	00
HOMO	-10.790	00	01	99	00	00
HOMO-1	-10.827	06	36	57	00	00
HOMO-2	-10.950	02	04	94	00	00
HOMO-3	-11.014	29	24	47	00	00
HOMO-4	-11.048	08	02	90	00	00
HOMO-5	-11.154	01	03	96	00	00

α-MO			
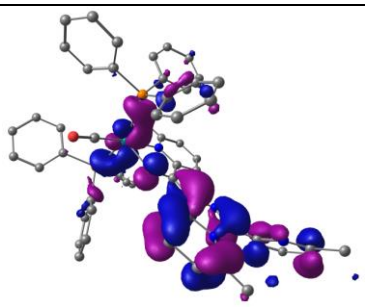	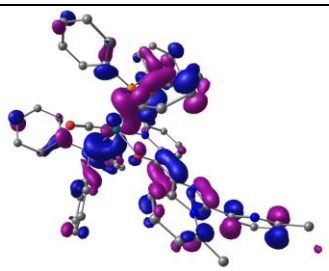	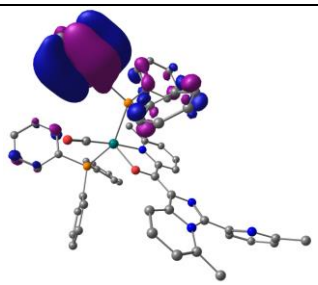	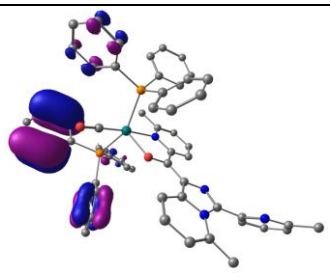
SOMO	HOMO-1	HOMO-2	HOMO-3
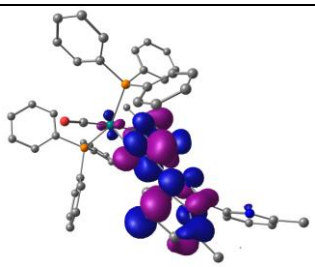	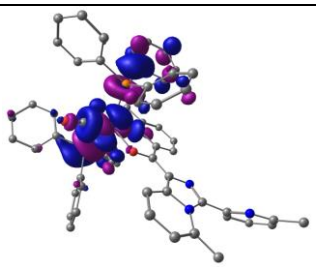	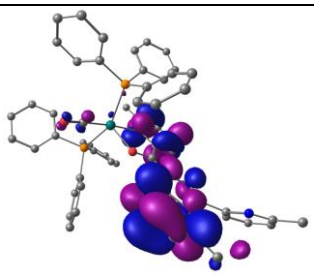	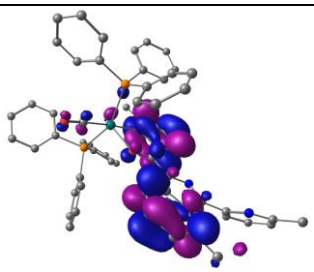
LUMO	LUMO+1	LUMO+2	LUMO+3
β-MO			
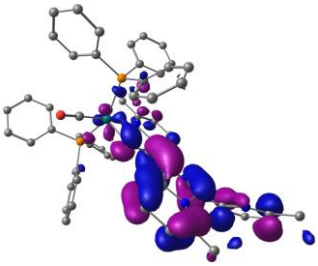	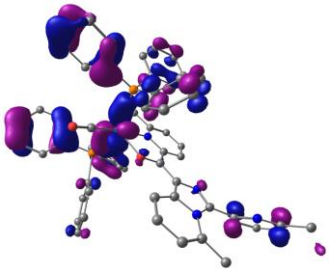	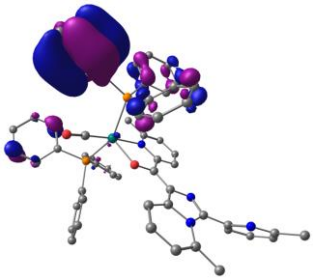	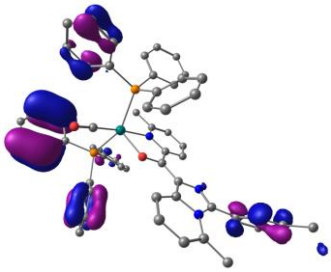
HOMO	HOMO-1	HOMO-2	HOMO-3
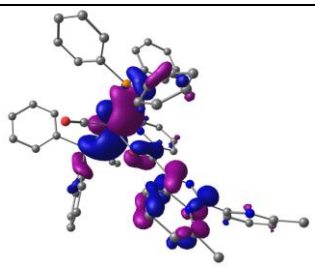	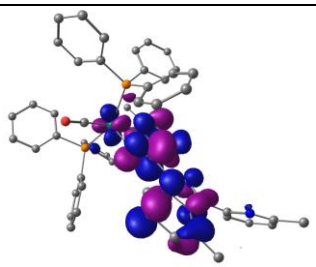	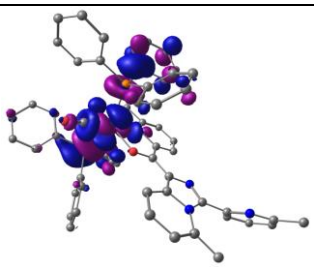	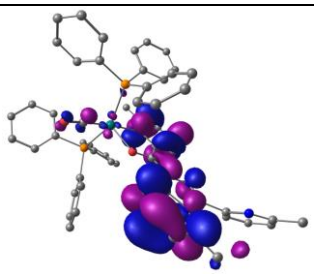
LUMO	LUMO+1	LUMO+2	LUMO+3

Table S14 DFT-calculated MO compositions for **2**$^{+}$ in S = 0 state

MO	Energy (eV)	% Composition				
		Ru	L2′	PPh_3	CO	H
LUMO+5	-2.662	01	85	14	00	00
LUMO+4	-2.944	26	05	67	01	00
LUMO+3	-3.094	01	92	06	01	00
LUMO+2	-3.251	00	99	00	01	00
LUMO+1	-3.433	02	94	03	01	00
LUMO	-4.652	05	86	09	00	00
HOMO	-7.676	35	45	19	00	00
HOMO-1	-8.213	10	24	66	01	00
HOMO-2	-8.310	72	11	06	10	00
HOMO-3	-8.353	61	20	18	02	00
HOMO-4	-8.556	04	02	93	00	00
HOMO-5	-8.587	16	06	77	01	00

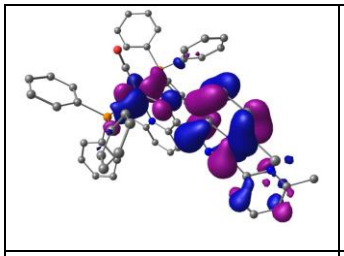	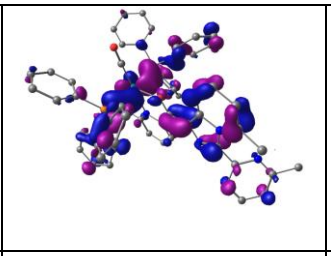	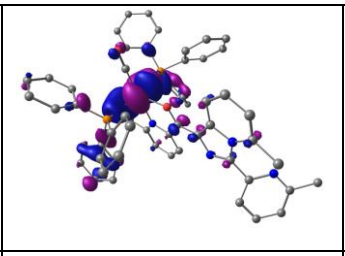	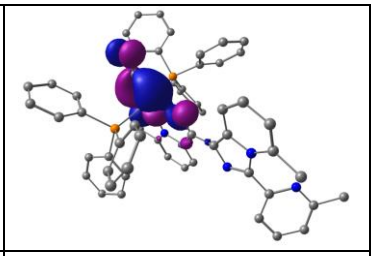
HOMO	HOMO-1	HOMO-2	HOMO-3
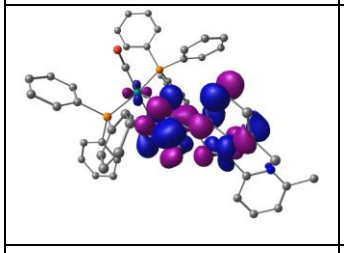	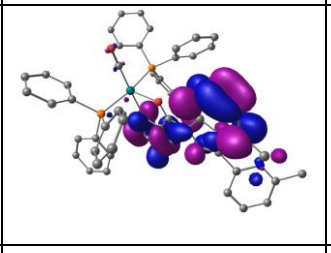	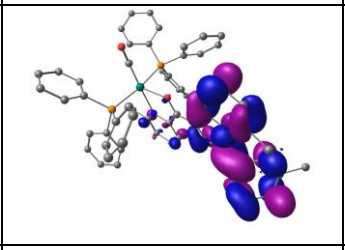	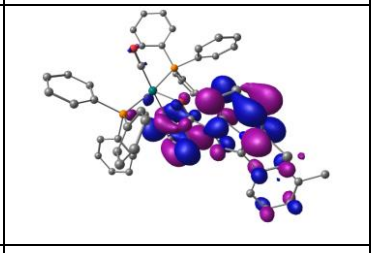
LUMO	LUMO+1	LUMO+2	LUMO+3

Table S15 DFT-calculated MO compositions for **2** in *S* = 1/2 state

MO	Energy (eV)	% Composition				
		Ru	L2′	PPh_3	CO	H
			α-MO			
LUMO+5	-0.235	04	04	91	01	00
LUMO+4	-0.285	03	81	16	01	00
LUMO+3	-0.353	11	04	84	01	00
LUMO+2	-0.404	02	06	91	02	00
LUMO+1	-0.524	19	77	03	00	00
LUMO	-0.811	00	99	01	00	00
SOMO	-2.334	05	85	10	00	00
HOMO-1	-4.656	19	70	11	00	00
HOMO-2	-5.356	56	27	07	08	01
HOMO-3	-5.441	60	21	17	03	00
HOMO-4	-5.702	44	06	47	02	00
HOMO-5	-6.036	30	17	48	04	00
			β-MO			
LUMO+5	-0.231	04	04	91	01	00
LUMO+4	-0.350	11	03	85	01	00
LUMO+3	-0.392	02	02	95	01	00
LUMO+2	-0.518	18	03	78	00	00
LUMO+1	-0.707	03	89	08	00	00
LUMO	-0.901	04	86	09	00	00
HOMO	-4.472	16	75	09	00	00
HOMO-1	-5.290	52	30	12	05	01
HOMO-2	-5.381	62	22	11	06	00
HOMO-3	-5.680	44	08	46	03	00
HOMO-4	-5.948	15	47	35	02	00
HOMO-5	-6.106	34	33	25	03	05

α-MO			
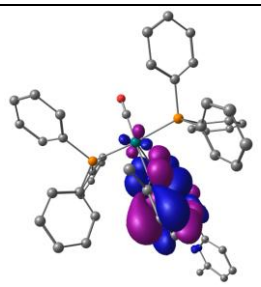	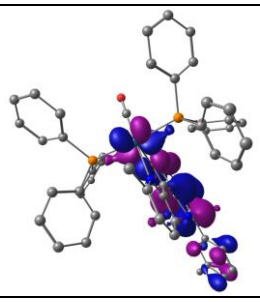	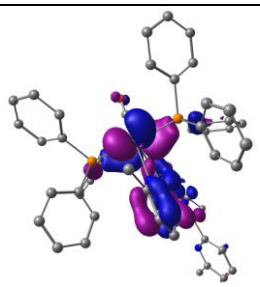	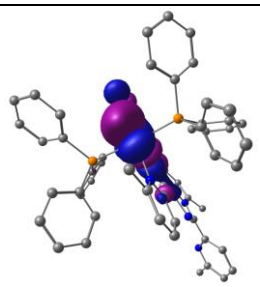
SOMO	HOMO-1	HOMO-2	HOMO-3
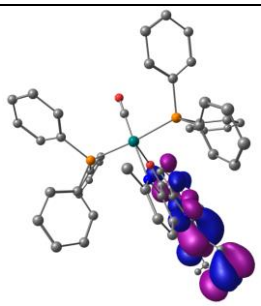	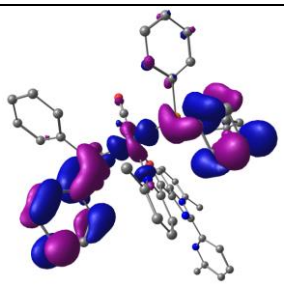	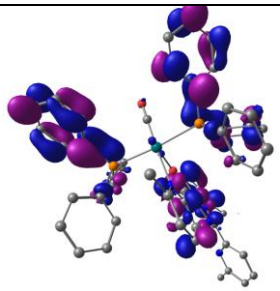	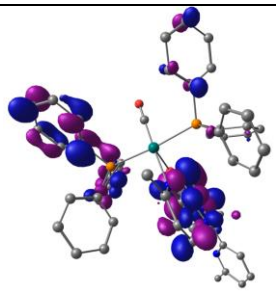
LUMO	LUMO+1	LUMO+2	LUMO+3
β-MO			
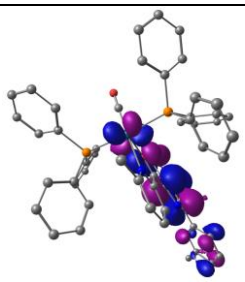	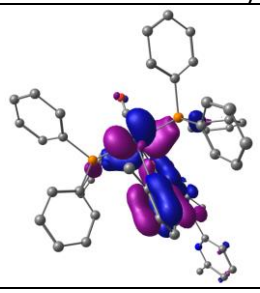	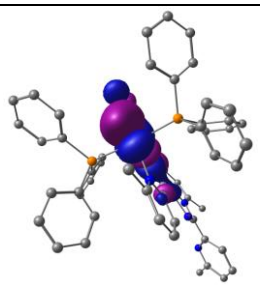	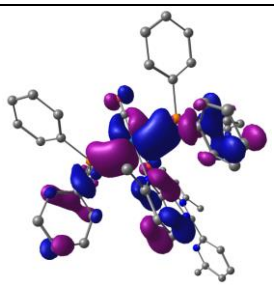
HOMO	HOMO-1	HOMO-2	HOMO-3
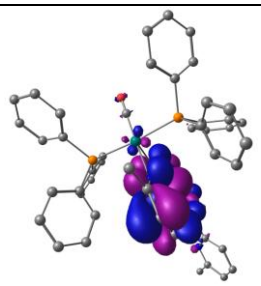	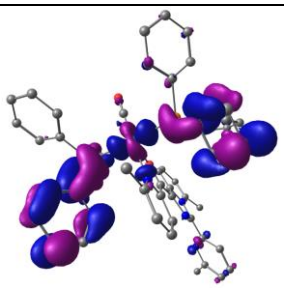	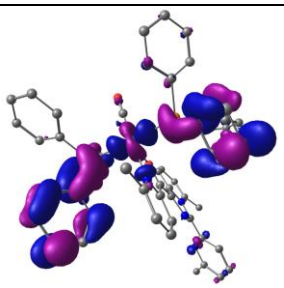	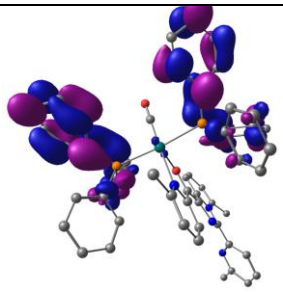
LUMO	LUMO+1	LUMO+2	LUMO+3

Table S16 DFT-calculated MO compositions for **3**$^{2+}$ in S = 1/2 state

MO	Energy (eV)	% Composition				
		Ru	L3′	PPh_3	CO	H
			α-MO			
LUMO+5	-5.781	08	75	17	01	00
LUMO+4	-5.938	12	67	19	02	00
LUMO+3	-6.056	26	15	56	02	01
LUMO+2	-6.555	05	85	09	00	00
LUMO+1	-6.661	01	96	03	01	00
LUMO	-7.808	03	91	05	00	00
SOMO	-11.089	06	22	72	00	00
HOMO-1	-11.205	01	28	70	00	00
HOMO-2	-11.257	01	15	84	00	00
HOMO-3	-11.308	01	30	69	00	00
HOMO-4	-11.352	01	02	97	00	00
HOMO-5	-11.380	02	10	88	01	00
			β-MO			
LUMO+5	-5.901	10	70	19	01	00
LUMO+4	-5.986	24	20	53	02	02
LUMO+3	-6.480	05	85	10	00	00
LUMO+2	-6.599	01	96	03	01	00
LUMO+1	-7.732	05	88	07	00	00
LUMO	-10.094	33	27	40	00	00
HOMO	-11.117	03	41	55	00	00
HOMO-1	-11.216	06	21	73	00	00
HOMO-2	-11.267	16	17	67	00	00
HOMO-3	-11.289	24	08	67	00	00
HOMO-4	-11.330	04	02	93	01	00
HOMO-5	-11.351	02	04	94	00	00

α-MO			
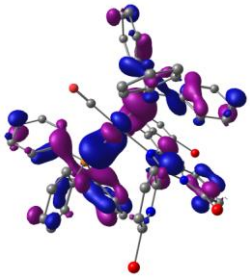	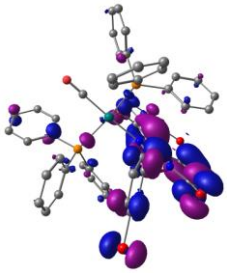	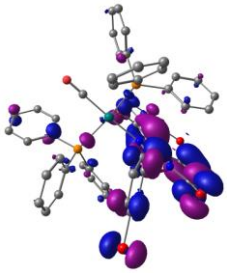	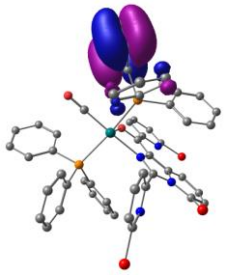
SOMO	HOMO-1	HOMO-2	HOMO-3
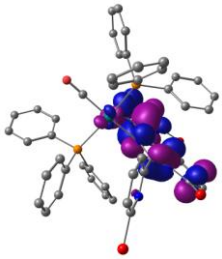	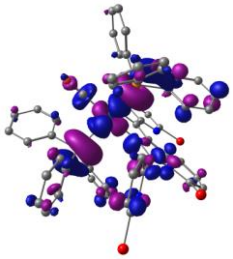	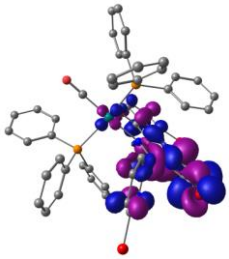	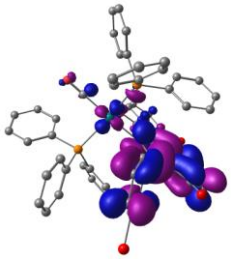
LUMO	LUMO+1	LUMO+2	LUMO+3
β-MO			
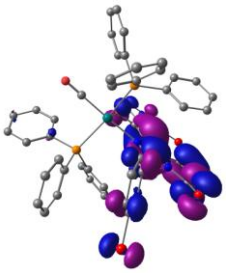	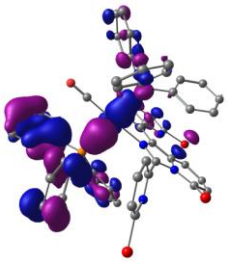	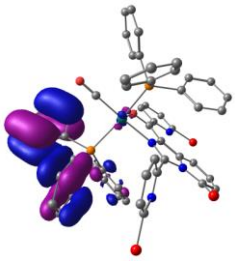	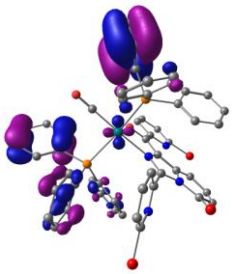
HOMO	HOMO-1	HOMO-2	HOMO-3
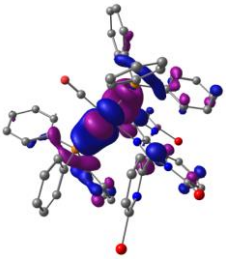	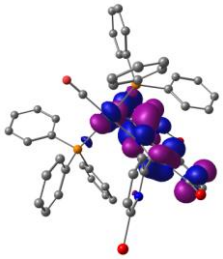	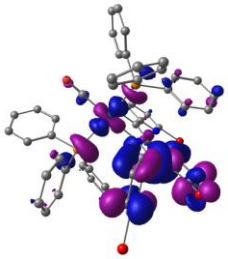	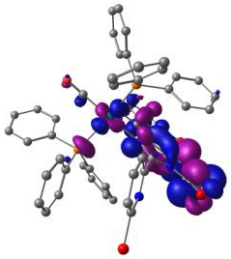
LUMO	LUMO+1	LUMO+2	LUMO+3

Table S17 DFT-calculated MO compositions for **3**$^{+}$ in S = 0 state

MO	Energy (eV)	% Composition				
		Ru	L3′	PPh_3	CO	H
LUMO+5	-3.101	23	10	66	01	00
LUMO+4	-3.308	05	79	15	01	00
LUMO+3	-3.477	01	96	03	00	00
LUMO+2	-3.825	03	89	07	00	00
LUMO+1	-3.950	01	97	02	00	00
LUMO	-5.036	04	90	06	00	00
HOMO	-8.165	27	30	42	00	00
HOMO-1	-8.518	33	16	50	01	00
HOMO-2	-8.574	50	36	11	03	00
HOMO-3	-8.704	60	17	13	10	00
HOMO-4	-8.752	08	04	87	01	00
HOMO-5	-8.836	12	03	84	01	00

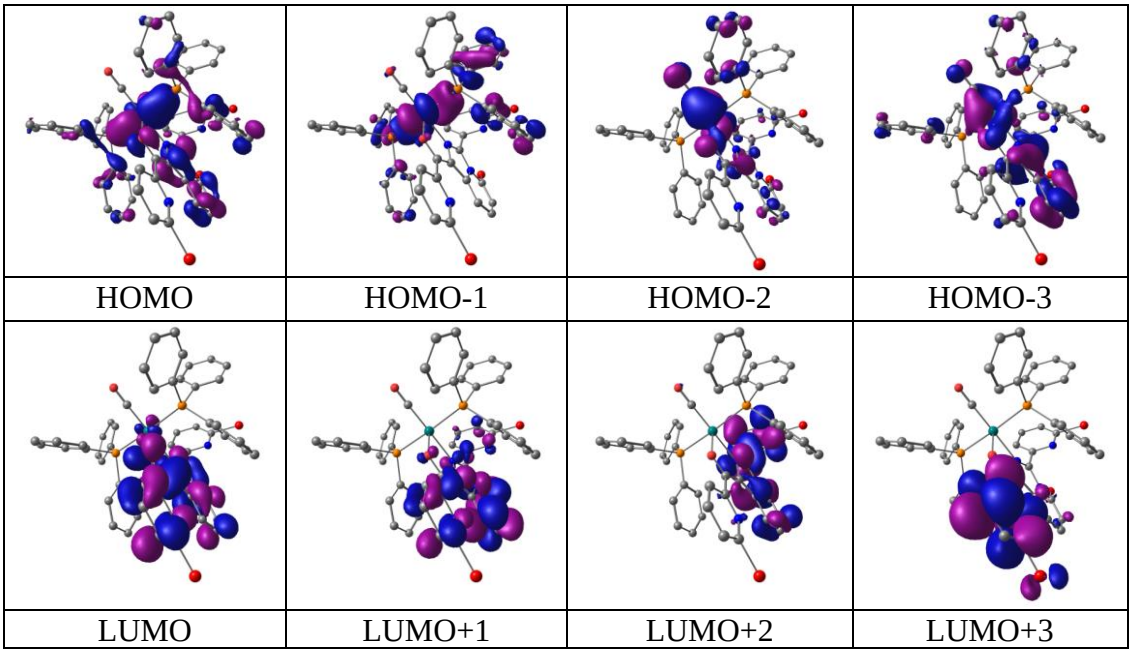

Table S18 DFT-calculated MO compositions for **3** in S = 1/2 state

MO	Energy (eV)	% Composition				
		Ru	L3′	PPh_3	CO	H
			α-MO			
LUMO+5	-0.483	02	08	90	00	00
LUMO+4	-0.597	20	20	59	01	00
LUMO+3	-0.811	07	63	27	01	01
LUMO+2	-0.867	03	07	90	00	00
LUMO+1	-0.880	01	92	07	00	00
LUMO	-1.210	04	85	11	00	00
SOMO	-2.739	04	89	06	00	00
HOMO-1	-5.303	15	72	13	00	00
HOMO-2	-5.713	47	30	22	02	00
HOMO-3	-5.881	63	20	05	12	00
HOMO-4	-5.953	44	09	46	02	00
HOMO-5	-6.311	20	41	35	03	01
			β-MO			
LUMO+5	-0.588	20	23	56	01	00
LUMO+4	-0.620	02	92	06	01	00
LUMO+3	-0.797	08	61	29	01	01
LUMO+2	-0.865	03	04	92	00	00
LUMO+1	-1.078	02	88	09	00	00
LUMO	-1.242	06	83	11	01	00
HOMO	-5.116	12	79	09	00	00
HOMO-1	-5.609	48	30	21	01	00
HOMO-2	-5.841	60	23	04	13	00
HOMO-3	-5.927	39	11	48	02	00
HOMO-4	-6.195	15	65	18	01	00
HOMO-5	-6.338	26	48	22	03	01

α-MO			
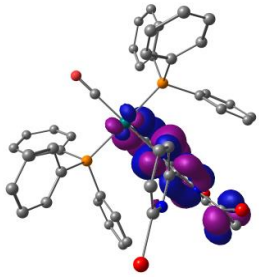	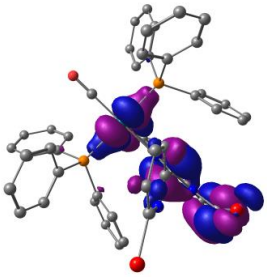	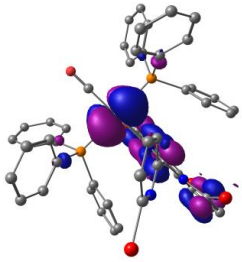	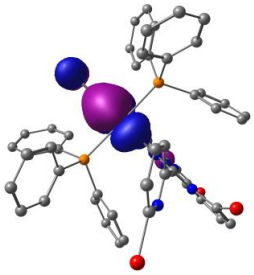
SOMO	HOMO-1	HOMO-2	HOMO-3
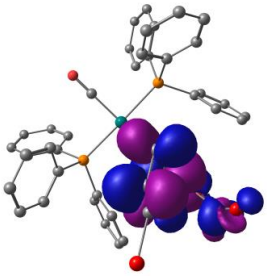	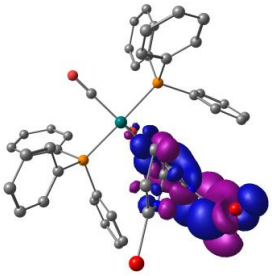	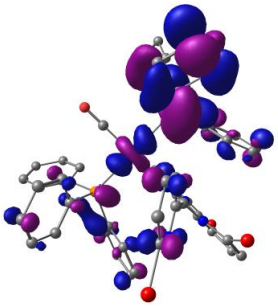	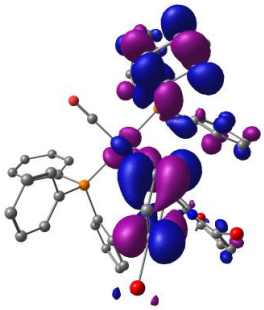
LUMO	LUMO+1	LUMO+2	LUMO+3
β-MO			
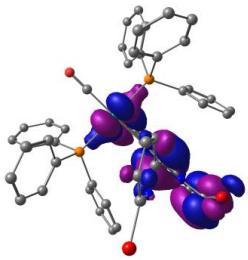	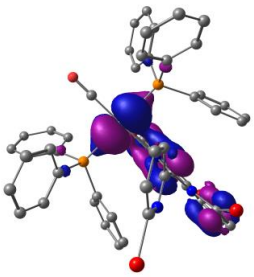	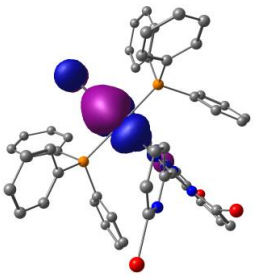	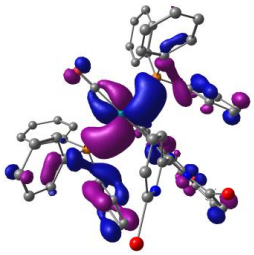
HOMO	HOMO-1	HOMO-2	HOMO-3
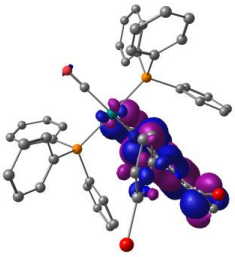	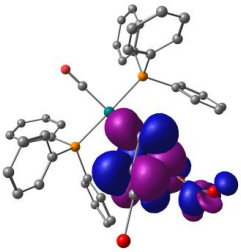	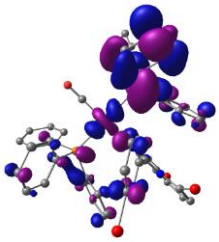	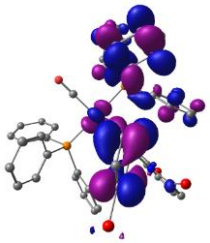
LUMO	LUMO+1	LUMO+2	LUMO+3

Table S19 DFT-calculated MO compositions for **3**$^{-}$ in S = 1 state

MO	Energy (eV)	% Composition				
		Ru	L3′	PPh_3	CO	H
			α-MO			
LUMO+5	2.012	10	02	86	01	00
LUMO+4	1.922	06	15	79	00	00
LUMO+3	1.865	05	06	88	00	00
LUMO+2	1.699	07	32	60	01	00
LUMO+1	1.644	08	55	35	01	00
LUMO	1.403	01	16	82	00	00
SOMO	0.943	11	50	39	00	00
HOMO-1	-0.273	04	90	06	00	00
HOMO-2	-2.619	11	80	09	00	00
HOMO-3	-3.170	63	19	16	02	00
HOMO-4	-3.326	68	16	04	12	00
HOMO-5	-3.388	36	17	45	03	00
			β-MO			
LUMO+5	1.975	03	22	75	00	00
LUMO+4	1.911	02	65	31	01	00
LUMO+3	1.868	10	09	81	00	00
LUMO+2	1.703	16	04	78	01	00
LUMO+1	1.567	03	03	94	01	00
LUMO	1.368	04	87	09	01	00
HOMO	-2.379	08	85	07	00	00
HOMO-1	-3.051	63	20	17	01	00
HOMO-2	-3.274	65	19	03	13	00
HOMO-3	-3.324	34	26	37	03	00
HOMO-4	-3.541	08	71	18	02	00
HOMO-5	-3.796	25	30	39	05	00

α-MO			
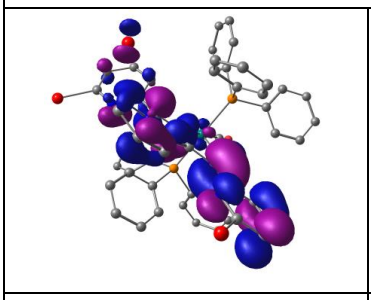	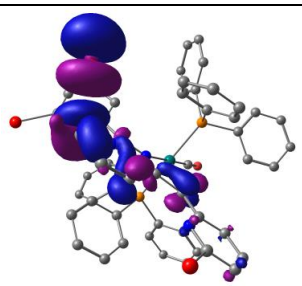	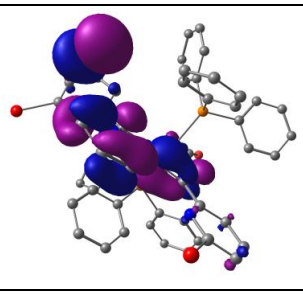	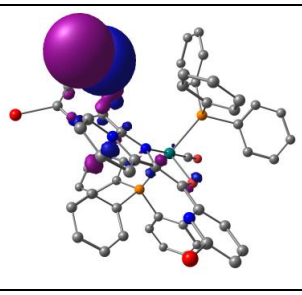
SOMO	HOMO-1	HOMO-2	HOMO-3
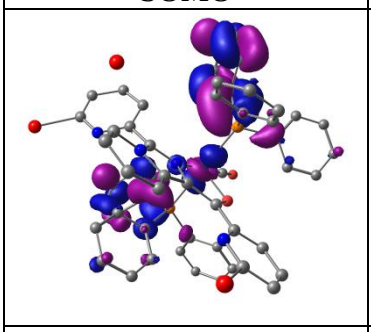	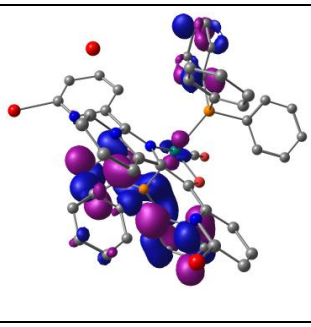	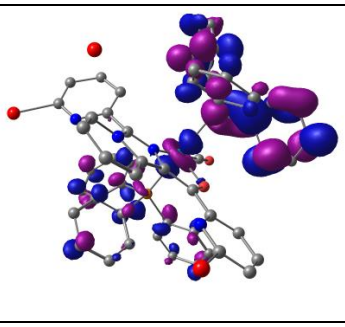	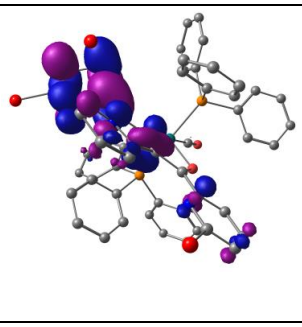
LUMO	LUMO+1	LUMO+2	LUMO+3
β-MO			
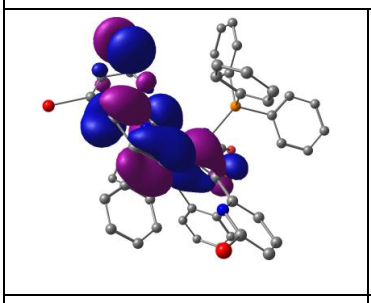	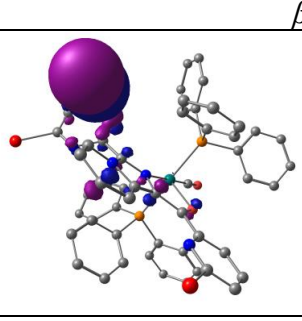	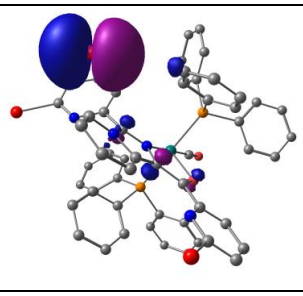	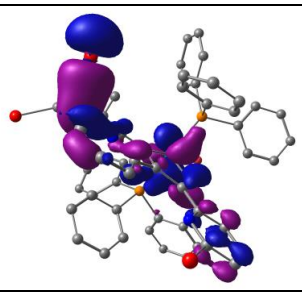
HOMO	HOMO-1	HOMO-2	HOMO-3
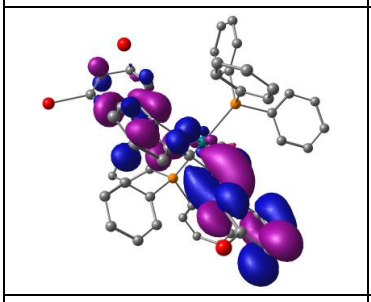	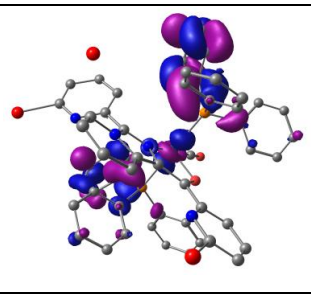	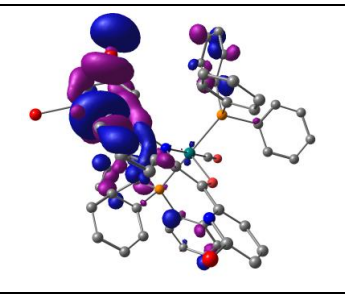	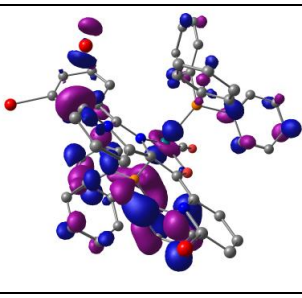
LUMO	LUMO+1	LUMO+2	LUMO+3

Table S20 DFT calculated selected MO compositions

Complex	MO	Fragments	% Contribution
1^{3+} (*S*=1/2)	*β*-LUMO	Ru/L1/PPh_3	03/83/12
1^{2+} (*S*=0)	HOMO LUMO	Ru/L1/PPh_3 Ru/L1/PPh_3	02/97/01 14/80/03
1^{+} (*S*=1/2)	SOMO *β*-LUMO	Ru/L1/PPh_3 Ru/L1/PPh_3	48/28/17 10/84/03
1 (*S*=1)	SOMO	Ru/L_1/PPh_3	14/70/10
2^{2+} (*S*=1/2)	*β*-LUMO	Ru/L2′/PPh_3	45/33/21
2^{+} (*S*=0)	HOMO LUMO	Ru/L2′/PPh_3 Ru/L2′/PPh_3	35/45/19 05/86/09
2 (*S*=1/2)	SOMO	Ru/L2′/PPh_3	05/85/10
3^{2+} (*S*=1/2)	*β*-LUMO	Ru/L3′/PPh_3	33/27/40
3^{+} (*S*=0)	HOMO LUMO	Ru/L3′/PPh_3 Ru/L3′/PPh_3	27/30/42 04/90/06
3 (*S*=1/2)	SOMO *β*-LUMO	Ru/L3′/PPh_3 Ru/L3′/PPh_3	04/89/06 06/83/11
3^{-} (*S*=1)	SOMO	Ru/L3′/PPh_3	11/50/39

Table S21 DFT calculated (UB3LYP/LanL2DZ/6-31G*) Mulliken spin densities

Complex	Ru1/Ru2	L1/L2′/L3′	PPh_3	H	CO	Cl
$\mathbf{1}^{3+}$ (*S*=1/2)	0.00/0.040	0.931	0.021	0.002	-0.002	0.008
$\mathbf{1}^{+}$ (*S*=1/2)	0.444/0.311	0.186	0.101	-0.061	-0.014	0.033
1 (*S*=1)	0.350/0.196	1.330	0.092	-0.012	0.003	0.044
$\mathbf{2}^{2+}$ (*S*=1/2)	0.606	0.157	0.278	-0.016	-0.025	-
2 (*S*=1/2)	0.004	0.992	0.008	-0.002	0.002	-
$\mathbf{3}^{2+}$ (*S*=1/2)	0.620	0.083	0.339	-0.016	-0.026	-
3 (*S*=1/2)	0.007	0.982	0.012	-0.002	0.001	-
$\mathbf{3}^{-}$ (*S*=1)	0.005	1.984	0.011	-0.002	0.002	-

Table S22 Comparison of TON of [**1**]$(ClO_4)_2$ with previously reported complexes

Sr. No.	Complex	Potential	FE (%)	TON	Ref.
1.	$[Fe(C_5(p\text{-}C_6H_4Br)_5)(CO)_2Br]$	−1.00 V *vs* Ag/AgCl	-	25	11
2.	$Ni(^{p\text{-}tbu}dhbpy)$	-1.9 V vs Fc/Fc^+	94	9.07	12
3.	$[Cu(L_1H_2)(ClO_4)]ClO_4$	−1.65 V vs Fc^+/Fc	81	73.00	13
4.	$[Ni(L^1)_2]$	−1.50 V vs Fc/Fc^+	67.56	23.95	14
5.	$[Co(DO)(DOH)pnBr_2]$	-0.78 V vs. Fc/0	-	40	15
6.	$[BzPy]_2[Ni(tdas)_2]$	−1.10V vs Ag/Agcl	-	2202.2	16
7.	Ni(abt)2	-1.64 V vs SCE	~80	6190	17
8.	$[Cu_2(TPy)]$	−1.16 V vs Fc^+/Fc	96	102	18
9.	[Ni(L)]	-1.01 V vs. Fc^+/Fc	94	37	19
10.	$[Ni(P^{Ph}{}_2N^{Ph})_2]^{2+}$	-1.13V vs Fc^+/Fc	99	11	20
11	$[Ru_2(OTf)(\mu\text{-}H)(Me_2dad)(dbcot)_2]$@CC	−300 mV vs RHE	86	5.5×10^3	21
12	Sb-Salen@CC	−1.4 V vs NHE	96.8	43.4 s^{-1} (TOF)	22
13	Ni(DPMDA)@CC	−2.31 V vs Fc/Fc^+	-	25,900 s^{-1} (TOF)	23
14	[**1**]$(ClO_4)_2$	0.45 V vs RHE	98.4	**2.74×10^5**	This work

$^{p\text{-}tbu}$dhbpy = 4-tert-butyl-2-2-[6-[6-(5-tert-butyl-2hydroxy-phenyl)-2-pyridyl}-2-pyridyl phenol

L_1H_2 = diacetyl-bis(N-4-methyl-3-thiosemicarbazone)

HL^1 = 1-((4-hydroxybutylimino)methyl)naphthalen-2-ol

$(DO)(DOH)_{pn}$ = $N^2,N^{2\prime}$-propanediylbis(2,3-butandione 2-imine-3-oxime)

BzPy = benzyl pyridinium and tdas = 1,2,5-thiadiazole-3,4-dithiolate

(abt) = 2-aminobenzenethiolate

(TPy) = triply fused porphyrin

L = thiosemicarbazone

$P^{Ph}{}_2N^{Ph}$ = 1,3,6-triphenyl-1-aza-3,6-diphosphacycloheptane

DPMDA=2,2’-((diphenylmethylene)bis(1H-pyrrole-5,2-diyl))bis

(methaneylylidene))bis(azaneylylidene))dianiline

Table S23a Optimised cartesian coordinates of N,O piconyl binding mode of [**2**]ClO_4 using (UB3LYP/LanL2DZ/6-31G*).

Cartesian Coordinates

Ru	11.012298000	1.674960000	5.233533000
P	10.720119000	1.159955000	2.859823000
P	11.452119000	1.865989000	7.633887000
O	9.683965000	3.464401000	5.145904000
N	12.322466000	3.442484000	4.792994000
O	9.023356000	-0.505848000	5.877108000
N	7.529251000	7.078216000	5.072270000
C	11.684142000	4.652361000	4.741812000
N	9.757273000	7.059686000	4.858558000
C	10.200930000	4.595432000	4.965893000
C	10.663964000	-0.646604000	2.470545000
C	7.934016000	5.734792000	5.101935000
C	13.065890000	2.637048000	8.108303000
C	11.477300000	0.238762000	8.513968000
C	9.802865000	0.316517000	5.627496000
C	10.208135000	2.850111000	8.581989000
C	13.655531000	3.394605000	4.581397000
C	8.867366000	2.811513000	8.167777000
H	8.595594000	2.253482000	7.278648000
C	13.249414000	4.022214000	7.951406000
H	12.432233000	4.643464000	7.596987000
C	12.030340000	1.801850000	1.724210000
C	6.975137000	4.713878000	5.231302000
H	7.314881000	3.688815000	5.215066000
C	11.389652000	-1.559623000	3.251553000
H	11.948526000	-1.203698000	4.110549000
C	9.343976000	5.758866000	4.976141000
C	9.935731000	-1.126004000	1.368679000
H	9.364307000	-0.440473000	0.751643000
C	11.390349000	-2.919578000	2.936005000
H	11.955419000	-3.613936000	3.551590000
C	9.140889000	1.785906000	2.126521000
C	10.659990000	-3.386468000	1.842467000
H	10.653753000	-4.445923000	1.602388000
C	6.732295000	2.042018000	2.354992000
H	5.830571000	1.920266000	2.948964000
C	14.387163000	4.563048000	4.312131000
H	15.456288000	4.484470000	4.147070000
C	12.961487000	0.942297000	1.121139000
H	12.895837000	-0.128676000	1.280829000
C	12.037457000	-0.884136000	7.882490000
H	12.413014000	-0.797325000	6.868228000
C	12.371270000	5.838128000	4.473988000

H	11.820736000	6.768042000	4.443565000
C	6.656897000	2.581089000	1.068775000
H	5.698041000	2.886070000	0.659211000
N	8.037391000	9.855642000	3.727529000
C	9.932812000	-2.486498000	1.060670000
H	9.359191000	-2.842556000	0.209570000
C	7.963805000	1.655261000	2.882744000
H	8.006342000	1.237944000	3.883270000
C	14.374910000	2.075415000	4.632403000
H	14.274681000	1.618288000	5.620149000
H	15.437953000	2.215839000	4.419065000
H	13.960765000	1.377985000	3.900098000
C	9.052569000	2.318957000	0.830760000
H	9.942292000	2.419163000	0.218725000
C	10.538874000	3.580918000	9.735860000
H	11.566786000	3.619437000	10.080850000
C	13.746677000	5.789578000	4.256865000
H	14.301913000	6.698924000	4.046352000
C	14.136092000	1.866186000	8.587275000
H	14.016095000	0.797415000	8.728932000
C	12.137095000	3.184127000	1.488677000
H	11.423221000	3.869951000	1.935320000
C	14.467715000	4.619057000	8.274265000
H	14.587303000	5.692880000	8.158786000
C	7.881165000	3.484604000	8.889680000
H	6.847944000	3.442932000	8.556689000
C	12.107950000	-2.110145000	8.545147000
H	12.545301000	-2.968533000	8.042856000
C	7.819309000	2.719353000	0.310154000
H	7.770343000	3.130823000	-0.694198000
C	10.980049000	0.102010000	9.820028000
H	10.537892000	0.951483000	10.328932000
C	9.551085000	4.259208000	10.452370000
H	9.822995000	4.819151000	11.342863000
C	15.527870000	3.841785000	8.747827000
H	16.476132000	4.307526000	9.000830000
C	13.972028000	1.452695000	0.302236000
H	14.681118000	0.771711000	-0.160086000
C	8.703727000	7.840500000	4.893543000
C	11.607530000	-2.236296000	9.842169000
H	11.653468000	-3.193185000	10.354337000
C	6.204196000	7.442389000	5.299759000
C	11.042207000	-1.128601000	10.475525000
H	10.645988000	-1.219347000	11.482978000
C	15.358543000	2.465710000	8.901447000
H	16.173736000	1.853636000	9.277067000
C	13.139913000	3.689572000	0.661817000
H	13.198324000	4.759259000	0.480326000
C	5.653246000	5.063239000	5.370037000

H	4.888898000	4.298358000	5.465303000
C	8.834185000	9.296502000	4.652341000
C	5.814856000	8.879851000	5.454219000
H	6.430927000	9.380653000	6.209950000
H	4.771098000	8.933755000	5.771443000
H	5.943417000	9.429010000	4.518246000
C	14.063034000	2.824799000	0.068113000
H	14.843896000	3.218608000	-0.576328000
C	8.220776000	4.212439000	10.031571000
H	7.453009000	4.738058000	10.592527000
C	8.222355000	11.148308000	3.411639000
C	5.285027000	6.427760000	5.427536000
H	4.250261000	6.701816000	5.600000000
C	9.858063000	9.995743000	5.304476000
H	10.478051000	9.495295000	6.039713000
C	9.226827000	11.919298000	4.014218000
H	9.355037000	12.959682000	3.731630000
C	10.050235000	11.334631000	4.973572000
H	10.830964000	11.914640000	5.457502000
C	7.287170000	11.731940000	2.382418000
H	7.102471000	11.009066000	1.582627000
H	7.688601000	12.651595000	1.947227000
H	6.316660000	11.972927000	2.835624000
H	12.152709000	0.559987000	5.240175000

Table S23b Optimised cartesian coordinates of N(imidazopyridine)/O(piconyl) binding mode of [**2**]ClO_4 using (UB3LYP/LanL2DZ/6-31G*).

Cartesian Coordinates

Ru	11.752422000	8.182362000	7.171009000
P	14.074988000	8.819467000	7.589326000
P	9.408770000	7.650283000	6.699941000
O	11.243822000	8.432411000	9.372131000
O	11.342603000	10.837880000	5.781144000
N	12.050243000	6.241080000	8.146007000
N	14.364768000	4.607011000	6.287367000
N	12.542498000	4.182828000	8.809735000
N	10.518245000	6.561854000	12.258065000
C	13.041214000	4.826787000	6.366275000
C	15.283202000	8.582349000	6.214731000
C	12.510240000	5.075736000	7.734920000
C	14.216988000	10.617906000	7.996814000
C	11.320936000	7.416321000	10.109540000
C	10.929942000	7.616972000	11.541233000
C	11.772142000	6.176897000	9.502793000
C	15.289858000	11.408062000	7.558660000
H	16.073177000	10.975988000	6.945323000
C	11.491955000	9.837167000	6.346193000
C	16.652790000	8.380603000	6.456557000
H	17.020875000	8.302194000	7.474295000
C	8.675990000	6.368075000	7.817920000
C	14.870329000	7.986414000	9.038209000
C	8.598899000	10.007719000	7.989187000
H	9.457591000	9.828310000	8.629244000
C	7.786131000	11.119063000	8.216195000
H	8.018444000	11.797813000	9.032306000
C	8.995775000	7.049313000	5.004126000
C	12.869223000	2.825879000	8.849967000
C	12.784287000	4.679104000	3.992382000
H	12.166858000	4.705986000	3.099275000
C	12.208746000	4.878260000	5.247029000
H	11.150526000	5.082891000	5.345801000
C	8.310469000	9.117568000	6.939427000
C	12.092223000	4.876136000	9.949270000
C	14.838261000	8.688296000	4.887881000
H	13.783369000	8.840420000	4.686854000
C	14.923353000	4.431961000	5.078165000
C	15.001034000	8.636286000	10.275147000
H	14.688312000	9.669176000	10.384728000
C	17.098812000	8.389422000	4.076304000
H	17.801012000	8.318142000	3.250270000
C	14.358321000	13.339467000	8.684111000

H	14.411234000	14.392795000	8.944406000
C	17.552670000	8.281623000	5.393071000
H	18.609164000	8.128937000	5.596086000
C	9.796855000	7.451114000	3.923223000
H	10.677036000	8.057618000	4.106932000
C	14.153718000	4.451690000	3.904751000
H	14.630946000	4.294268000	2.942339000
C	8.899590000	5.000917000	7.575947000
H	9.426789000	4.683560000	6.681708000
C	13.287327000	12.560421000	9.127119000
H	12.503054000	13.006480000	9.732781000
C	15.305651000	6.653626000	8.924458000
H	15.226124000	6.122308000	7.980256000
C	15.740471000	8.595314000	3.827168000
H	15.380473000	8.684723000	2.805957000
C	15.861709000	5.996427000	10.022463000
H	16.203886000	4.970637000	9.913331000
C	7.860904000	6.259044000	4.748185000
H	7.221930000	5.941539000	5.565972000
C	13.212010000	11.211006000	8.780727000
H	12.369070000	10.613182000	9.114576000
C	8.419133000	4.031899000	8.456318000
H	8.586258000	2.979660000	8.241789000
C	15.985719000	6.650620000	11.250791000
H	16.423070000	6.137336000	12.102713000
C	9.472664000	7.071717000	2.619232000
H	10.098711000	7.398116000	1.793292000
C	12.835258000	2.207053000	10.073178000
H	13.090158000	1.154054000	10.116718000
C	10.087713000	6.752891000	13.514627000
C	15.355982000	12.760788000	7.898756000
H	16.188819000	13.361940000	7.544937000
C	10.946673000	8.922001000	12.052396000
H	11.285069000	9.742980000	11.433022000
C	12.070397000	4.207590000	11.190107000
H	11.713206000	4.754410000	12.048889000
C	7.963663000	6.735133000	8.969830000
H	7.764428000	7.781437000	9.175301000
C	15.553498000	7.971081000	11.372663000
H	15.655660000	8.494454000	12.319440000
C	7.543999000	5.874548000	3.444168000
H	6.665155000	5.261921000	3.263570000
C	6.687357000	11.366373000	7.391076000
H	6.061738000	12.237890000	7.561719000
C	8.348612000	6.279651000	2.377050000
H	8.098364000	5.982192000	1.362589000
C	12.458053000	2.893853000	11.251458000
H	12.449640000	2.365777000	12.199554000
C	7.203412000	9.373441000	6.116191000

H	6.966659000	8.708732000	5.292523000
C	10.070890000	8.028140000	14.099475000
H	9.716240000	8.152879000	15.118099000
C	7.713936000	4.410419000	9.601304000
H	7.335706000	3.655030000	10.284254000
C	7.488649000	5.763228000	9.853650000
H	6.931666000	6.069060000	10.734789000
C	10.515455000	9.121433000	13.360685000
H	10.518560000	10.116519000	13.796154000
C	6.400423000	10.493070000	6.341192000
H	5.551121000	10.682342000	5.690772000
H	12.167898000	7.679517000	5.723589000
C	13.207367000	2.072083000	7.598185000
H	14.163613000	2.394882000	7.178665000
H	13.267319000	1.007654000	7.835687000
H	12.446283000	2.207162000	6.822309000
C	16.418118000	4.242974000	5.040832000
H	16.752229000	3.642984000	5.892264000
H	16.740653000	3.759737000	4.113953000
H	16.921340000	5.215931000	5.106462000
C	9.640262000	5.530219000	14.276858000
H	8.965640000	5.791495000	15.097233000
H	9.133082000	4.829058000	13.608235000
H	10.502299000	5.008171000	14.713082000

Table S23c Optimised cartesian coordinates of N(imidazopyridine)/O(piconyl) binding mode of [**3**]ClO_4 using (UB3LYP/LanL2DZ/6-31G*).

Cartesian Coordinates

Ru	11.405047000	8.839617000	6.907574000
Br	12.445510000	2.439221000	6.871447000
Br	10.336235000	5.937152000	14.560737000
Br	16.489304000	4.456404000	5.086515000
P	13.724835000	9.485975000	7.342171000
P	9.078229000	8.275828000	6.381772000
O	10.881629000	9.055320000	9.097822000
O	10.973292000	11.509932000	5.553257000
N	11.701359000	6.892630000	7.869397000
N	14.019810000	5.145891000	6.132352000
N	12.076961000	4.792420000	8.462046000
N	10.644452000	7.239583000	12.134909000
C	12.717269000	5.485824000	6.088526000
C	14.931398000	9.248096000	5.969316000
C	12.104738000	5.721385000	7.420408000
C	13.865701000	11.281732000	7.756552000
C	10.993521000	8.050513000	9.843336000
C	10.665244000	8.279212000	11.286646000
C	11.424717000	6.803594000	9.225806000
C	14.937601000	12.070777000	7.313806000
H	15.717534000	11.637275000	6.697144000
C	11.132137000	10.502580000	6.102671000
C	16.295792000	9.015228000	6.211993000
H	16.659593000	8.911836000	7.228900000
C	8.365544000	6.949974000	7.459249000
C	14.500276000	8.639654000	8.793016000
C	8.203893000	10.605701000	7.682365000
H	9.074804000	10.454956000	8.313014000
C	7.356538000	11.689229000	7.917667000
H	7.573045000	12.375881000	8.731515000
C	8.712458000	7.706226000	4.664606000
C	12.286104000	3.420606000	8.474107000
C	12.699626000	5.422643000	3.697158000
H	12.184683000	5.531607000	2.747356000
C	12.016065000	5.645696000	4.894980000
H	10.974732000	5.940042000	4.892494000
C	7.937717000	9.707904000	6.633781000
C	11.679855000	5.472629000	9.635399000
C	14.492363000	9.385508000	4.642887000
H	13.442214000	9.565884000	4.440270000
C	14.644010000	4.943659000	4.987823000
C	14.607188000	9.275125000	10.039852000
H	14.292327000	10.306758000	10.155712000

C	16.748274000	9.049803000	3.834238000
H	17.450579000	8.971008000	3.009177000
C	14.013001000	14.002228000	8.444745000
H	14.068184000	15.055268000	8.705584000
C	17.195355000	8.911826000	5.149477000
H	18.245973000	8.725010000	5.352536000
C	9.510104000	8.172170000	3.606606000
H	10.360910000	8.810877000	3.818379000
C	14.041579000	5.058102000	3.729918000
H	14.608791000	4.871183000	2.826118000
C	8.632714000	5.595264000	7.191609000
H	9.178666000	5.311916000	6.296863000
C	12.943434000	13.224012000	8.892710000
H	12.163205000	13.670707000	9.503102000
C	14.940666000	7.309337000	8.672188000
H	14.886143000	6.790293000	7.720358000
C	15.396053000	9.291089000	3.584043000
H	15.041884000	9.405477000	2.563235000
C	15.477872000	6.638826000	9.771322000
H	15.826627000	5.616524000	9.652779000
C	7.613597000	6.879130000	4.370584000
H	6.977438000	6.512714000	5.169807000
C	12.865205000	11.875011000	8.545774000
H	12.024405000	11.277464000	8.885824000
C	8.173441000	4.594989000	8.048591000
H	8.374414000	3.552917000	7.814744000
C	15.576996000	7.278565000	11.009557000
H	15.999845000	6.756188000	11.863172000
C	9.218317000	7.817680000	2.288108000
H	9.840503000	8.193248000	1.480410000
C	12.265966000	2.744757000	9.662548000
H	12.435986000	1.675449000	9.653701000
C	10.344483000	7.459740000	13.398781000
C	15.006586000	13.423129000	7.654529000
H	15.838669000	14.023518000	7.297821000
C	10.376488000	9.583162000	11.710304000
H	10.403129000	10.398401000	10.999583000
C	11.647041000	4.758846000	10.850821000
H	11.351940000	5.291288000	11.741044000
C	7.631115000	7.273340000	8.610723000
H	7.398400000	8.309580000	8.832852000
C	15.140562000	8.597088000	11.139111000
H	15.225706000	9.109407000	12.093585000
C	7.329225000	6.520529000	3.051743000
H	6.478410000	5.878612000	2.841458000
C	6.243144000	11.899881000	7.102188000
H	5.590184000	12.749774000	7.278975000
C	8.130516000	6.988167000	2.008112000
H	7.905748000	6.710252000	0.982271000

C	11.971322000	3.425430000	10.866479000
H	11.960370000	2.873859000	11.800650000
C	6.815891000	9.927501000	5.819813000
H	6.595920000	9.256972000	4.996254000
C	10.039590000	8.716068000	13.931171000
H	9.800758000	8.832417000	14.981444000
C	7.446258000	4.929681000	9.193743000
H	7.084728000	4.150426000	9.858520000
C	7.176392000	6.270074000	9.470033000
H	6.599880000	6.539923000	10.350487000
C	10.061580000	9.795484000	13.052058000
H	9.835309000	10.794674000	13.412128000
C	5.977091000	11.018483000	6.053383000
H	5.116564000	11.179768000	5.410328000
H	11.848846000	8.365538000	5.459485000

Table S24d Optimised cartesian coordinates of N,O piconyl binding mode of [**3**]ClO_4 using (UB3LYP/LanL2DZ/6-31G*).

Cartesian Coordinates

Ru	11.070446000	1.522723000	5.350713000
P	10.759270000	1.030759000	2.974752000
P	11.513744000	1.722388000	7.749965000
O	9.809907000	3.377744000	5.244281000
N	12.448421000	3.267919000	4.907130000
O	9.088173000	-0.651610000	6.008799000
N	7.776478000	7.058309000	5.175942000
C	11.849778000	4.502203000	4.858400000
N	10.001225000	6.970316000	4.983508000
C	10.363543000	4.488813000	5.074241000
C	10.772726000	-0.764890000	2.540110000
C	8.134407000	5.697194000	5.185157000
C	13.091728000	2.565744000	8.219900000
C	11.606094000	0.094604000	8.622758000
C	9.857584000	0.178052000	5.751399000
C	10.227274000	2.654898000	8.693717000
C	13.765526000	3.213454000	4.697058000
C	8.894986000	2.598842000	8.254869000
H	8.649161000	2.054405000	7.349868000
C	13.198428000	3.963446000	8.107689000
H	12.339806000	4.553947000	7.801390000
C	12.020115000	1.764926000	1.841916000
C	7.136629000	4.707760000	5.248771000
H	7.442038000	3.672234000	5.209477000
C	11.516162000	-1.673131000	3.309366000
H	12.051068000	-1.321400000	4.184848000
C	9.545616000	5.683200000	5.085304000
C	10.076985000	-1.238832000	1.414843000
H	9.491212000	-0.556961000	0.807228000
C	11.566243000	-3.023850000	2.959324000
H	12.144433000	-3.715152000	3.566048000
C	9.140538000	1.609915000	2.287119000
C	10.868928000	-3.485506000	1.842446000
H	10.901524000	-4.537939000	1.575221000
C	6.729390000	1.787145000	2.568303000
H	5.845069000	1.628913000	3.179908000
C	14.560973000	4.335968000	4.433079000
H	15.624316000	4.211422000	4.272268000
C	13.009273000	0.972076000	1.242069000
H	13.018495000	-0.100505000	1.404075000
C	12.228357000	-0.995727000	7.991942000
H	12.616090000	-0.884146000	6.984699000
C	12.576044000	5.664099000	4.598050000

H	12.055331000	6.611191000	4.570329000
C	6.607975000	2.329680000	1.287039000
H	5.631068000	2.604650000	0.899552000
N	8.302867000	9.711224000	3.751646000
C	10.124336000	-2.589811000	1.071899000
H	9.575938000	-2.942310000	0.202913000
C	7.984227000	1.437399000	3.067119000
H	8.058585000	1.013403000	4.062735000
C	9.005028000	2.144931000	0.995819000
H	9.876777000	2.276289000	0.364156000
C	10.521435000	3.364210000	9.871094000
H	11.542384000	3.415929000	10.234662000
C	13.951650000	5.577643000	4.383690000
H	14.535282000	6.469940000	4.178790000
C	14.212344000	1.837466000	8.644536000
H	14.153439000	0.759319000	8.747588000
C	12.033011000	3.151796000	1.609540000
H	11.267857000	3.784965000	2.049557000
C	14.392652000	4.612752000	8.419307000
H	14.452712000	5.694989000	8.340810000
C	7.881976000	3.233533000	8.974756000
H	6.855163000	3.175357000	8.624508000
C	12.346140000	-2.222096000	8.647008000
H	12.831902000	-3.054769000	8.145949000
C	7.748570000	2.508003000	0.504127000
H	7.664636000	2.921636000	-0.496970000
C	11.094606000	-0.075637000	9.919152000
H	10.603553000	0.747275000	10.426760000
C	9.507221000	4.004180000	10.585642000
H	9.751307000	4.547608000	11.494190000
C	15.503313000	3.876985000	8.840538000
H	16.432357000	4.383165000	9.087059000
C	13.984397000	1.551135000	0.426566000
H	14.739844000	0.920929000	-0.034142000
C	8.972852000	7.783493000	5.013126000
C	11.831154000	-2.382016000	9.934620000
H	11.913750000	-3.339756000	10.440510000
C	6.461743000	7.430964000	5.403621000
C	11.204182000	-1.307314000	10.566537000
H	10.796160000	-1.424767000	11.566469000
C	15.408697000	2.489805000	8.951540000
H	16.263994000	1.909293000	9.285603000
C	13.003224000	3.726566000	0.788944000
H	12.988306000	4.797810000	0.607116000
C	5.820870000	5.095074000	5.342802000
H	5.028143000	4.354853000	5.375141000
C	9.109633000	9.222809000	4.711337000
C	13.983930000	2.926839000	0.196099000
H	14.737924000	3.373636000	-0.445770000

C	8.185680000	3.940197000	10.139737000
H	7.397148000	4.435399000	10.699479000
C	8.468930000	10.969845000	3.394792000
C	5.489027000	6.466680000	5.454983000
H	4.465682000	6.776335000	5.626191000
C	10.110910000	9.980332000	5.323856000
H	10.738732000	9.540011000	6.090138000
C	9.432189000	11.828152000	3.937487000
H	9.515051000	12.853174000	3.597198000
C	10.267300000	11.308308000	4.922532000
H	11.028246000	11.935498000	5.377572000
H	12.169973000	0.382947000	5.360005000
Br	6.011160000	9.212252000	5.808360000
Br	7.299824000	11.643171000	2.038955000
Br	14.675440000	1.549437000	4.738952000

References

1 N. Ahmad, J. J. Levison, S. D. Robinson, M. P. Uttley, E. R. Wonchoba and G. W. Parshall, *Inorg. Synth.*, 2007, **15**, 45-64.

2 (*a*) N. Kundu, K. Bhattacharya, T. M. S. Abtab and M. Chaudhury, *Tetrahedron Lett.*, 2012, **53**, 2719-2721; (*b*) N. Kundu, T. M. S. Abtab, S. Kundu, A. Endo and S. J. Chaudhury, *Inorg. Chem.*, 2012, **51**, 2652-2661; (*c*) N. Kundu, M. Maity, P. B. Chatterjee, J. S. Teat, A. Endo and M. Chaudhury, *J. Am. Chem. Soc.*, 2011, **133**, 20104-20107.

3 (*a*) G. M. Sheldrick, *Acta Crystallogr. Sect.* A. 2008, **A64**, 112-122; (*b*) *Program for Crystal Structure Solution and Refinement; University of Göttingen: Göttingen, Germany,* 1997; (*c*) G. M. Sheldrick, *Acta Crystallogr. Sect. C: Struct. Chem.*, 2015, **C71**, 3-8.

4 C. Lee, W. Yang and R. G. Parr, *Phys. Rev., B* 1988, **37**, 785-789.

5 (*a*) D. Andrae, U. Haeussermann, M. Dolg, H. Stoll and H. Preuss, *Theor. Chim. Acta.*, 1990, **77**, 123-141; (*b*) P. Fuentealba, H. Preuss, H. Stoll and L. von Szentpaly, *Chem. Phys. Lett.*, 1989, **89**, 418-422.

6 (*a*) R. Bauernschmitt and R. Ahlrichs, *Chem. Phys. Lett.*, 1996, **256**, 454-464; (*b*) R. E. Stratmann, G. E. Scuseria and M. J. Frisch, *J. Chem. Phys.*, 1998, **109**, 8218-8225; (*c*) M. E. Casida, C. Jamorski, K. C. Casida and D. R. Salahub, *J. Chem. Phys.*, 1998, **108**, 4439-4450.

7 (*a*) V. Barone and M. Cossi, *J. Phys. Chem.*, A 1998, **102**, 1995-2001; (*b*) M. Cossi and V. Barone, *J. Chem. Phys.*, 2001, **115**, 4708-4718; (*c*) M. Cossi, N. Rega, G. Scalmani and V. Barone, *J. Comput. Chem.*, 2003, **24**, 669-681.

8 S. I. Gorelsky, *SWizard program*, http://www.sg-chem.net/.

9 S. Leonid, *Chemissian 1.7*, **2005-2010.** Available at http://www.chemissian.com.

10 D. A. Zhurko and G. A. Zhurko, *ChemCraft 1.5*, Plimus, San Diego, CA. Available at http://www.chemcraftprog.com.

11 E. B. Hemminga, B. Chanb, C. P. Turner, A. L. Corcilius, J. R. Pricec, D. M. G. Gardiner, A. A. F. Masters and T Maschmeyer, *Appl. Catal. B: Environ.*, 2018, **223**, 234-241.

12 J. M. Dressel, E. N. Cook, S. L. Hooe, J. J. Moreno, D. A. Dickie and C. W. Machan, *Inorg. Chem. Front.*, 2023, **10**, 972-978.

13 A. Z. Haddad, S. P. Cronin, M. S. Mashuta, R. M. Buchanan and C. A. Grapperhaus, *Inorg. Chem.*, 2017, **18**, 11254-11265.

14 A. Barma, M. Chakraborty, S. K. Bhattacharya P. Ghosh and P. Roy, *Mater. Adv*., 2022, **3**, 7655-7666.

15 P. A. Jacques, V. Artero, J. P. Cautb and M. Fontecavea, *PNAS*. 2009, **49**, 20627-20632.

16 Z. Niu, L. Yang. Y. Xiao, M. Xue1, J. Zhou, L. Zhang, J. Zhang, D. P. Wilkinson and C. Ni, *Electrocatalysis*, 2022, **13**, 230-241.

17 A. Das, Z. Han, W. W. Brennessel, P. L. Holland and R. Eisenberg. *ACS Catal*., 2015, **5**, 1397-1406.

18 S. Chandra, A. S. Hazari, Q. Song, D. Hunger, N. I. Neuman, J. V. Slageren, E. Klemm and B. Sarkar, *ChemSusChem.* 2023, **16**, e202201146.

19 M. Papadakis, A. Barrozo, T. Straistari, N. Queyriaux, A. Putri, J. Fize, M. Giorgi, M. Réglier, J. Massin, R. Hardré and M. Orio, *Dalton Trans*., 2020, **16**, 5064-5073.

20 M. L. Helm, M. P. Stewart, R. M. Bullock, M. R. Dubois and D. L. Dubois, *Science*, 2011, **333**, 863-866.

21 M. Bellini, J. Bösken, M. Wörle, D. Thöny, J. J. Gamboa-Carballo, F. Krumeich, F. Bàrtoli H. A. Miller, L. Poggini, W. Oberhauser, A. Lavacch, H. Grützmacher and F. Vizza, *Chem. Sci*., 2022, **13**, 3748-3760.

22 C. K .Williams, G. A . McCarver, A. Chaturvedi, S. Sinha, M. Ang, K. D Vogiatzis, and J. J. Jiang, *Chem. Eur. J*., 2022, **28**, p.e202201323.

23 L. Trowbridge, B. Averkiev, and P. E. Sues, *Chem. Eur. J*., 2022, **28**, p.e202301920.